



HHS Public Access

Author manuscript

Sci Transl Med. Author manuscript; available in PMC 2021 February 09.

Published in final edited form as:

Sci Transl Med. 2020 November 25; 12(571): . doi:10.1126/scitranslmed.aaw0285.

Sampling interstitial fluid from human skin using a microneedle patch

Pradnya P. Samant¹, Megan M. Niedzwiecki^{2,3}, Nicholas Raviele¹, Vilinh Tran⁴, Juan Mena-Lapaix¹, Douglas I. Walker^{2,3,4}, Eric I. Felner⁵, Dean P. Jones⁴, Gary W. Miller², Mark R. Prausnitz^{1,*}

¹School of Chemical and Biomolecular Engineering, Georgia Institute of Technology, Atlanta, GA 30332

²Department of Environmental Health, Emory University, Atlanta, GA 30322

³Department of Environmental Medicine and Public Health, Icahn School of Medicine at Mount Sinai, New York, NY 10029

⁴Clinical Biomarkers Laboratory, Division of Pulmonary, Allergy, Critical Care and Sleep Medicine, Emory University, Atlanta, GA 30322

⁵Department of Pediatrics, Division of Endocrinology, Emory University School of Medicine, Atlanta, GA 30322

Abstract

Tissue interstitial fluid (ISF) surrounds cells and is an under-utilized source of biomarkers that complements conventional sources like blood and urine. However, ISF has received limited attention due largely to lack of simple collection methods. Here, we developed a minimally invasive, microneedle-based method to sample ISF from human skin that was well tolerated by participants. Using a microneedle patch to create an array of micropores in skin coupled with mild suction, we sampled ISF from 21 human participants and identified clinically-relevant and sometimes distinct biomarkers in ISF when compared to companion plasma samples based on mass spectrometry analysis. Many biomarkers used in research and current clinical practice were common to ISF and plasma. Because ISF does not clot, these biomarkers could be continuously monitored in ISF similar to current continuous glucose monitors, but without requiring an indwelling subcutaneous sensor. Biomarkers distinct to ISF included molecules associated with systemic and dermatological physiology as well as exogenous compounds from environmental exposures. We also determined that pharmacokinetics of caffeine in healthy adults and pharmacodynamics of glucose in children and young adults with diabetes were similar in ISF and

*Corresponding author. prausnitz@gatech.edu.

Author contributions: PPS, MMN, DPJ, GM, and MRP designed the experiments. PPS, NR, JMP performed the human experiments. JML performed the animal experiments. MMN, VT, DIW performed the mass spectrometry experiments. PPS performed all the other analytical assays. PPS, MMN, VT, JML, DIW, DPJ, GM, MRP performed data analysis and contributed to its interpretations. PPS, MMN, GM, MRP wrote the manuscript in consultation with all authors.

Competing interests: MRP is an inventor of patents licensed to companies developing microneedle-based products, is a paid advisor to companies developing microneedle-based products and is a founder/shareholder of companies developing microneedle-based products (Micron Biomedical). This potential conflict of interest has been disclosed and is managed by Georgia Tech and Emory University. PPS and MRP are inventors on a patent application (WO2019126735A1) submitted by Georgia Tech Research Corporation that covers ISF collection methods presented in this study.

plasma. Overall, these studies provide a minimally invasive method to sample dermal ISF using microneedles and demonstrate human ISF as a source of biomarkers that may enable research and translation for future clinical applications.

One sentence summary

Interstitial fluid from skin sampled with a microneedle-based method identified clinically-relevant metabolic biomarkers in humans compared to plasma.

Introduction:

Identification and measurement of biomarkers have increasing importance in advancing research and detecting and treating diseases (1, 2). Biomarkers are molecules found in body fluids such as blood, urine, and saliva that provide information about physiological status. Diagnosis and monitoring are central to effective healthcare; for example, diabetes management by blood glucose testing, quick detection of infectious diseases like HIV and ability to characterize cancers by blood sampling. Blood monitoring is limited by the need for expert training, difficulty of continuous monitoring, and pain and apprehension associated with blood draws (3). Urine and saliva are more accessible but have limited biomarkers and variable concentrations (4).

The most prevalent accessible fluid in the body is interstitial fluid (ISF), constituting 75% of extracellular fluid and 15–25% of body weight. ISF surrounds cells and tissues, acting as a bridge between blood and cells (5). It contains systemic biomarkers and can also be used for continuous monitoring. ISF contains local tissue biomarkers that can provide information about cellular and tissue physiology (6). Previous studies have shown that ISF contains information similar to plasma (7, 8) as well as distinct biomarkers not otherwise found in plasma (9).

Currently, ISF is used clinically for continuous glucose monitoring (10) and in research to determine dermatological drug bioavailability (11) and analysis of cancer tumor microenvironment (12). More widespread use of ISF is limited because ISF is difficult to sample. In the skin, which is the most accessible organ of the body, ISF is mostly present in the lowermost skin layer of dermis, which is 70% ISF by volume (13). Dermal ISF can be sampled by biopsy, but it is painful, requires medical expertise, can lead to scarring, and collects a mixture of extracellular ISF and intracellular material (14). Alternatively, suction blisters, created by applying suction to the skin for approximately one hour at elevated temperature, are filled with ISF. However, this procedure is cumbersome, uncomfortable for the participant, can cause lasting skin damage, and provides fluid contaminated with injury markers not representative of physiologic ISF (15).

Microdialysis and open-flow microperfusion require implantation of a semipermeable membrane or steel-mesh tubing into skin, often under local anesthesia, which causes tissue damage and requires multiple hours to perform, and collected analytes are limited by the permeability of the membrane (16, 17). Reverse iontophoresis uses electric current to draw ISF components towards the skin surface, but is limited to collection of small molecules,

may irritate skin and requires frequent calibration because of skin permeability variation (18). Alternatively, biosensors placed inside the body provide in situ measurement in ISF, for example for continuous glucose monitoring (10). However, this requires a dedicated, implanted sensor for a given biomarker and risks infection, biofouling, and discomfort of an indwelling device.

An ideal system to sample ISF should reliably collect 1 μ L of ISF, which is sufficient for multiple analytical assays; be minimally invasive to avoid artifacts due to tissue damage or irritation; and be simple and rapid, requiring 20 min to perform to facilitate access and throughput. We hypothesized that these criteria could be met using microneedles (MN), which are micron-scale needles that press into skin, penetrate the outer skin barrier, and access dermal ISF in a minimally invasive manner. MNs have been studied clinically for drug delivery applications and are well tolerated and easy to use, making them well-suited for routine use in research and medicine (19). There has been developing interest in the use of MN-based devices to sample ISF through skin, however many previous studies of MNs for ISF sampling have been limited by sub-microliter sampling volumes.

In this study, we developed a MN-based method, in conjunction with a standard vacuum pump and commercially available gauze, to sample microliter volumes of ISF from skin in a minimally-invasive manner. We assessed acceptability of this method by studying skin tolerability, pain, and patients' opinions. The utility of ISF collected in this way was studied by comparing our results against ISF collection from suction blisters and plasma collection by venipuncture. We analyzed the ISF for biomarkers of clinical interest and/or biomarkers distinct to dermal ISF, and compared pharmacokinetics of caffeine and pharmacodynamics of glucose as model biomarkers in ISF versus plasma to assess potential future clinical value of ISF sampling.

Results

Design of microneedle patch to sample interstitial fluid

We designed an ISF collection method that uses MNs to create pathways for ISF flow from skin using vacuum as a convective driving force. Prior approaches have used solid, swellable MNs, which are limited in ISF collection by MN volume (20), and hollow MNs that collect biomarkers by diffusion or convection of ISF by capillary action, which are slow and/or collect small ISF volumes (21). These prior methods provide a driving force for ISF flow within MNs, but rely on slow diffusion of ISF through dermis to the dermis-MN interface. In our design, vacuum application initiates a convective driving force that moves ISF through the dermis to the skin surface via MN-generated pathways. These micropores are created by pressing a patch containing an array of five MNs into the skin and then removing it multiple times (Fig. 1A). Vacuum is applied over micropores to transport ISF through the dermis and micropores to the skin surface (fig. S1).

A challenge when collecting ISF is preventing contamination with blood. Because skin is highly vascularized, vacuum application to skin punctured with MNs can collect blood along with ISF. We therefore studied the effect of MN length, vacuum pressure, and timing of vacuum application in human participants. Since blood vessels are present to a greater extent

deeper in dermis(13), more shallow depth of MN insertion and weaker vacuum should reduce bleeding. We found that insertion of MN of three different lengths (250 μm , 450 μm and 650 μm) followed immediately by application of vacuum at -34 kPa or -50 kPa (gauge) resulted in bleeding onto the skin surface (fig. S2). Vacuum at -17 kPa (gauge) also led to bleeding when preceded by treatment with 650 μm long MNs, but the chances of bleeding decreased at shorter MN lengths, although 40% of participants still bleed when using 250 μm MNs (fig. S2). We did not reduce MN length below 250 μm because insertion of shorter MNs into skin is unreliable due to skin elasticity during insertion (22) and can require the use of a high-velocity applicator (23).

As a further attempt to eliminate bleeding, we delayed the onset of vacuum application in order to let broken capillaries reseal through the process of blood coagulation that starts within a few seconds (24). Delaying application of vacuum at -50 kPa (gauge) for up to 10 min had no effect on bleeding; 7–8 μL of blood came out with little or no ISF (fig. S3A). We finally tried to slowly increase the vacuum from 0 kPa to -50 kPa (gauge) over the course of ~ 3 min. This optimized method collected 2.3 ± 2.6 μL clear ISF with no visual traces of blood within 20 min, and was used in all subsequent studies.

We expect that MNs inserted close to their full length (250 μm) although the penetration depth measurements were not made. Because minor bleeding was seen if vacuum application was not ramped or delayed, this observation is consistent with crossing the avascular epidermis (50 – 100 μm thick) and reaching blood vessels in the superficial dermis, which was the target skin layer for ISF collection.

Intra-subject and inter-subject variability was observed in the amount of fluid collected (fig. S4). We also found that ISF collection varied dramatically among individual micropores in an array that all received the same MN and vacuum treatment, such that the large majority of micropores remained dry. The heterogeneity of micropores with blood is probably due to the small odds of a given MN hitting a capillary to cause highly localized bleeding at the site of the micropore. The cause of heterogeneity of micropores producing ISF is less clear.

Collection of ISF from human participants

We collected ISF from 21 human participants (10 males and 11 females aged 28 ± 7 years, table S1). The procedure involved covering skin with a transparent film skin dressing (Tegaderm) containing 1-cm diameter openings where MN treatment was performed (Fig. 1). Insertion and removal of MNs was well tolerated with faint visual evidence of micropores in skin (Fig. 1B). After administration of vacuum over the micropores for up to 20 min, skin appearance was largely unchanged (Fig. 1C). Closer examination revealed droplets of ISF on the skin surface (Fig. 1D). Collection and examination of ISF showed it was clear with a slight yellow tinge. One day later, the skin generally showed no evidence of MN treatment, indicating swift recovery (Fig. 1E,F).

For comparison, we used an established method to collect ISF from suction blisters by applying vacuum at 40°C for up to 1 h, which separated epidermis from dermis and filled the resulting blister with fluid. Draining the blister with a needle and syringe collected suction blister fluid (SBF), which was similar in appearance to ISF collected by MN (Fig.

1G). Consistent with literature (25), suction blister treatment caused local erythema and edema, which resolved within a few days, and in some cases induced prolonged skin hyperpigmentation. Compared to MN treatment, suction blister treatment was observed to cause more severe and longer-lived tissue trauma, was more cumbersome and time-consuming to perform, and produced ISF that likely includes artifacts due to tissue injury.

Although MN treatment did not induce apparent adverse effects to skin, we carried out histopathological analysis of skin biopsies from hairless rats exposed to the MN application and/or vacuum treatment to further assess safety. Visual observation of rat skin after MN treatment showed slight swelling and erythema that resolved within a few hours. Compared to control samples (no treatment, Fig. 2A), examination of histopathological tissue sections by a board-certified dermatopathologist revealed minor focal inflammation at 4 h after MN treatment (Fig. 2B) that resolved within 24 h (Fig. 2C). The samples with MN application only (no vacuum treatment) showed no signs of inflammation. Interestingly, the skin sites only exposed to vacuum application showed signs of epidermal thinning 24 h after vacuum application. This may have occurred because vacuum application in the absence of MN pores may have caused the epidermis to start separating from the dermis (i.e., beginning of blister formation) (fig. S5).

Unique and clinically relevant biomarkers in ISF

We collected ISF from MN treatment, SBF from suction blisters and plasma from venipuncture from the cohort of 21 participants to compare biomarker compositions of the three fluids. High-quality data were available for 20 participants from high-resolution metabolomics using liquid chromatography-mass spectrometry (LC-MS) (table S2). This analysis detected 10,338 m/z features with hydrophilic interaction chromatography (HILIC), which provides improved detection of polar compounds, and 7,703 m/z features with reverse-phase C18 chromatography, which better detects lipophilic compounds (Fig. 3). Among m/z features found in HILIC, 63% were common to all three body fluids; 79% were common to plasma and ISF, suggesting that these metabolite measurements in ISF may be a surrogate for plasma; and 1% were unique to ISF. Similar data were obtained from C18 chromatography with 50% features common to all three body fluids; 60% common to plasma and ISF. However, 14% of features were unique to ISF, indicating that C18 chromatography provided better detection of ISF-specific metabolites. This is consistent with observations in our prior work that compared composition of SBF and plasma (26).

Comparing the m/z features found in ISF or SBF, only 72% were common to both fluids using HILIC chromatography and 64% features were common to both fluids using C18 chromatography, which demonstrates that ISF and SBF are not identical fluids, probably because of their different methods of sampling.

To better interpret differences between ISF and SBF, a swab was wiped across intact skin and analyzed for biomarkers. Because ISF was collected from the skin surface, it may contain more epidermal and skin surface biomarkers than SBF. Consistent with this expectation, among 8,020 m/z features detected in the skin swab in HILIC, 90% and 87% were also found in ISF and SBF, respectively. Differences were more apparent for C18, with 93% of skin swab m/z features also found in ISF, but only 68% also found in SBF (fig. S6).

To address possible contamination of ISF with skin surface biomarkers, we determined that the average biomarker had a signal ~8 times greater in ISF compared to skin swab. Additional analysis showed that 65% of features had signals >2-fold larger in ISF compared to skin swab and 51% of features had signals >4-fold higher in ISF compared to skin swab (table S3). This analysis suggests that many biomarkers can be measured in ISF without considerable interference from skin surface biomarkers, but that in some cases the signal from some biomarkers may be influenced or even dominated by the skin surface.

It should also be noted that 70% (HILIC) and 46% (C18) of features detected in skin swabs were also found in plasma (figs. S7 and S8), indicating that biomarkers found on the skin surface are not necessarily contaminants. Indeed, prior studies have shown that dermal and systemic biomarkers can be collected from the skin surface (27). It is unclear, however, if the source of biomarkers found on the skin swab is associated with endogenous metabolism of the skin, systemic biomarkers from dermal ISF, or from the environment. Additional studies are needed to better understand differences between ISF and SBF, and the role of epidermal and skin surface biomarkers. We conducted a targeted evaluation of medically relevant biomarkers in ISF, SBF and plasma. From a metabolite reference standard library, 170 metabolites were detected in at least one fluid (table S4); Table 1 shows a truncated list. Many biomarkers (49%) were found with high frequency (presence in >18/20 samples) in all three fluids. Only 3 biomarkers (2%) were frequently detected in plasma but not in ISF, which further emphasizes that ISF contains many of the same biomarkers as plasma. In contrast, 12% of biomarkers were commonly found in ISF but not in plasma, which shows that ISF also contains distinct information.

Reference standardization was used to estimate concentrations of 65 select biomarkers in ISF, SBF, and plasma (28, 29). About 50% of the biomarker concentrations were similar in ISF and plasma (within 3x of plasma concentration) (table S5). However, certain biomarkers, including amino acids such as serine, taurine, and ornithine, were markedly higher in ISF, consistent with previous reports comparing amino acid concentrations in plasma and skin-derived samples (30).

We further studied biomarkers that were frequently found in ISF and generally absent in plasma (Table 2). Among 26 clinically significant biomarkers, 13 were not frequently present (i.e., in <50% of samples) in SBF, possibly because they were more prevalent in epidermis or skin surface. Ten of these 13 biomarkers were also commonly detected in the skin swab, supporting this hypothesis. We also found 4 biomarkers in SBF that were not found in ISF (table S6). Of note are corticosterone, which activates in the skin in response to inflammation and other stressors (31), and 11-deoxycortisol, a cortisol precursor. This indicates that SBF may contain artifacts that result from tissue trauma inherent to the suction blister sampling method.

At the end of each study procedure, participants were asked questions about pain and tolerability. We found that ISF collection was well tolerated. Participants reported that pain during MN treatment was not different from suction blister or venipuncture, whereas suction blister sampling was significantly more painful than venipuncture (fig. S9A). Ongoing pain after the procedure was reported by almost half of participants with suction blisters, but only

by 5% after ISF collection using MNs (fig. S9B). Tenderness was reported by 70% of participants at suction blister sites, but only 24% after MN treatment. Erythema was seen at 89% of suction blister sites, split between grade 1 and grade 2 in severity, whereas erythema at MN sites was less common (76%) and less severe (all grade 1) (table S7). Localized swelling observed at 40% of suction blister sites and 57% of MN sites was always contained within the 1-cm² sites of vacuum application. Overall, ISF collection using MNs was well tolerated and generally had fewer adverse effects compared to suction blisters.

Monitoring systemic biomarker pharmacokinetics in ISF and plasma

Our measurements so far compare the presence of biomarkers in different body fluids, but do not address dynamic relationships as biomarkers are transported between body compartments. We therefore studied pharmacokinetics of a model biomarker (caffeine) in ISF compared to plasma over an 8 h period. Caffeine is a small, hydrophilic molecule expected to transport and equilibrate easily between blood and ISF (32), can be safely and easily administered to human participants, and its pharmacokinetics are well known (33).

ISF and blood were sampled by MN treatment and fingerstick, respectively, in 9 healthy adult subjects (table S8) who had abstained from caffeine consumption for 36 h. Baseline caffeine concentrations in ISF and plasma in all participants were below 0.5 µg/mL, consistent with expected values >24 h after caffeine abstention (34). After consuming a soft drink (Diet Coke) containing 43 mg of caffeine, caffeine concentrations in ISF and plasma increased for ~2 h and then decayed until the end of the 8 h study (Fig. 4A). There was a correlation between caffeine in ISF and blood ($r^2=0.73$, Fig. 4B), with a mean ISF/blood ratio of 0.95 ± 0.52 . Caffeine pharmacokinetic parameters were not significantly different when sampled in plasma or ISF ($p>0.05$, Fig. 4C) and are consistent with literature values (35). Possible lag in caffeine concentration in ISF relative to plasma was not seen or analyzed here due to the limited number of sampling time points (36, 37). Three participants later drank a caffeine-free Diet Coke soft drink, which resulted in caffeine concentrations in ISF and plasma below 0.25 µg/mL at all times (Fig. 4A). These caffeine concentrations are significantly lower than those measured when subjects consumed the caffeinated soft drink (t-test, $p<0.001$).

Sensations reported by participants were similar for MN and fingerstick; most participants reported slight or very slight sensations of pain and stinging (figs. S10 and S11). ISF collection by MNs induced mild erythema localized at the treatment sites that disappeared within a few days (figs. S12 and S13A). No post-procedure pain or swelling was reported. In contrast, fingerstick did not cause erythema but resulted in mild tenderness that disappeared with a few days (figs. S12 and S13B).

Monitoring glucose pharmacodynamics in ISF and plasma in participants with type 1 diabetes

We next studied the pharmacodynamic response of an ISF biomarker in a clinical population. Fifteen children and young adults with type 1 diabetes (table S9) were given a standard meal, after which insulin was administered and glucose monitored in ISF collected by MN and plasma by intravenous catheter for 3 h. In current clinical practice, glucose is

measured in subcutaneous ISF, but that requires an indwelling catheter. MNs could enable glucose monitoring in a minimally-invasive manner, which would be especially valuable in children, who have particularly poor compliance with glucose monitoring (38).

We found that the procedures in this study in children and young adults were well tolerated and pain scores reported by participants after ISF collection by MN patch were similar to those associated with finger-stick blood collection and significantly less than those associated with intravenous blood collection (fig. S14).

Clarke error grid analysis shows that points in the A+B region totaled 90% when 0.6 μL of ISF was collected, which shows good correlation (Fig. 5). However, ISF sample volumes collected in this study were low, and only 76% of points were in the A+B region when 0.25 μL of ISF was collected. Further analysis showed that the trends of glucose concentration in ISF generally followed plasma over time (fig. S15), but the correlation between ISF and plasma glucose concentration became weaker when collected ISF volume was lower (ANOVA, $p = 0.002$, fig. S16). This relationship is probably due to smaller signal-to-noise ratio when assaying smaller ISF volumes (i.e., containing less glucose) (See subsection on Variability of ISF volume collected).

Determination of ISF volume

Because knowing ISF volume is critical to determining biomarker concentration, we performed additional analysis on this topic. The ISF volume extracted was calculated by measuring the amount of sodium in a sample and normalizing by sodium concentration. This method relies on the expectation that sodium ion concentration is relatively constant in the body fluids of healthy participants, which is consistent with prior studies using sodium concentration in dermal ISF as an internal standard (39, 40) and formed the basis for development of a FDA-approved device measuring concentration of glucose collected from ISF by iontophoresis (GlucoWatch Biographer, Cygnus) (41). This method, however, comes with limitations of not having a direct measurement of ISF volume and may lead to inaccuracies if a subject has abnormal sodium levels or if sodium levels were altered by the ISF collection method. Prior studies have indicated that sodium reservoirs are found in the skin, largely bound to extracellular matrix, and can be released in ISF under certain conditions (42). Studies also suggest that there can be gradients in sodium concentration within the skin (43).

To address this issue, we carried out a study in which we collected ISF using a different method that determines ISF volume independent of sodium concentration and thereby directly measured sodium concentration in ISF collected from skin of rats before and after application of vacuum for 20 min, as used in this study (See subsection on Measurement of sodium concentration in rat ISF in Supplemental Materials). We found that ISF sodium concentration was 137 ± 17 mmol/L (mean \pm SD) before application of vacuum and 162 ± 18 mmol/L after application of vacuum. These measurements are not significantly different (Student's t-test, $p > 0.10$) given the variability of the data. The average ratio of ISF sodium concentration before and after vacuum application in paired experiments was 1.18 ± 0.31 . A ratio of 1 is within the 95% confidence interval (0.97 – 1.40), which indicates that this ratio is not significantly different than 1, again indicating that there is no significant difference in

ISF sodium concentration before and after ISF collection in this study. If future work were to identify a significant increase in sodium concentration, this could alter osmotically driven flow of ISF in the skin, which could in turn alter ISF composition (44). More studies are needed to understand the effect of ISF collection method on local concentration of sodium and more fully validate the sodium-based approach to ISF volume determination.

Variability of ISF volume collected

The total volume of ISF collected in this study showed variability. The average ISF volume collected in the caffeine study was $3.4 \pm 3.2 \mu\text{L}$, which is not significantly different compared to the ISF volume collected in the ISF collection optimization study, $2.3 \pm 2.6 \mu\text{L}$ (Student's t-test, $p > 0.05$), but the ISF volumes collected in the glucose study ($0.7 \pm 1.4 \mu\text{L}$) were considerably smaller (fig. S4) ($p < 0.0001$, unpaired t-test).

We hypothesized that variability might be correlated with sample size, where smaller ISF sample sizes might have more experimental noise. In the caffeine study, where volumes $>1 \mu\text{L}$ were usually collected, we investigated whether there was a correlation between the absolute percent difference in caffeine concentration measured in ISF versus plasma and the ISF volume collected, but we did not find a significant correlation (fig. S17) (two-way ANOVA, $p > 0.1$).

In the glucose study, in which ISF volumes were smaller, we found that correlation of ISF glucose concentrations with plasma glucose concentrations was significantly worse when ISF volume was small, as discussed above (Fig. 5). An estimation of the variance, bias, and irreducible error revealed that the irreducible error was higher for paired glucose values where ISF collected was $< 0.6 \mu\text{L}$ compared to those where the collected ISF volumes were $> 0.6 \mu\text{L}$ (table S10). This indicates that the noise in the dataset was reduced as ISF sample volume increased. The squared estimation bias was also much lower for samples where ISF volume collected was $> 0.25 \mu\text{L}$. This strengthens the hypothesis that the worse fit of glucose concentration in ISF with serum at lower ISF volumes discussed above is due at least in part to the noise from the sampling and analytical methods.

Discussion

ISF is a body fluid of increasing interest as a source of biomarkers providing information about both dermal and systemic physiology as well as drug pharmacokinetics. Unlike blood, ISF does not clot – making it potentially useful for continuous monitoring of biomarkers (45). However, progress in ISF monitoring has been limited by lack of simple, rapid, reliable and minimally invasive methods to sample ISF. Current methods include suction blisters (15), microdialysis (16, 46) and open flow microperfusion (17) which require expert training, take one or more hours to complete, cause skin injuries that require days to weeks to fully heal and often require local anesthesia due to their invasive nature.

Previous studies have demonstrated use of MNs to sample ISF. However, hollow MNs using capillary forces to draw ISF (47–49) and hydrogel MNs that swell with ISF upon insertion into skin (50, 51) have generally collected sub-microliter ISF volumes, which is less than required for most diagnostic tests (21). There have been prior approaches that have

successfully collected microliter volumes of ISF, such as a hydrogel MN patch made of crosslinked hyaluronic acid was found to collect $>1 \mu\text{L}$ within minutes (52). Solid, metal MNs have recently been shown to collect microliters of ISF, especially when skin was pre-treated to induce mild, local edema (53, 54). Other studies using small hypodermic needles and annular rings that apply pressure to the skin surface around each needle have collected microliters of ISF (55–57). Micropores have also been created in the skin by thermal ablation and successfully used to collect ISF to monitor glucose, cortisol and other analytes (58, 59).

Here, we developed an ISF collection method using the combination of MNs to create pathways for ISF transport and a standard vacuum pump to provide a driving force that draws ISF from skin, building off our prior work in this area (48, 60). Since the MNs are minimally invasive and the method uses equipment that is commercially available at relatively low cost, we believe this method can be broadly useful to the scientific community to collect ISF. In its current form, this technique may be less amenable to widespread clinical use because of the need for expert training and use of specialized equipment. However, with modifications to the equipment to make it smaller and simpler to use, future clinical communities could collect useful quantities of ISF (i.e., $1 \mu\text{L}$) using a minimally invasive method that is well-tolerated and relatively rapid and simple to do.

In this study, we analyzed ISF, SBF and plasma from 20 human participants and found more than 10,000 features by untargeted LC-MS analysis, most of which were common to ISF and plasma. This indicates that ISF may be a surrogate for plasma for at least some biomarkers. Further inspection showed that 94% of features found in plasma using HILIC chromatography (which captures more polar compounds) were also found in ISF. In comparison, 84% features were found in common between plasma and ISF using reverse phase C18 chromatography (which better detects lipophilic compounds). This indicates that hydrophilic compounds may be able to equilibrate more easily between ISF and plasma than hydrophobic compounds.

Additionally, more features unique to ISF were detected using the C18 column compared to using HILIC (14% vs. 1%, respectively). Skin may contain more unique lipophilic molecules as a result of endogenous cellular metabolic processes that are captured better by C18 compared to HILIC. One possible explanation for the presence of ISF-specific m/z features could be due to loss of sensitivity for these features in serum from increased matrix effects during measurement. However, if this is the case, it further highlights the use of ISF for monitoring low-concentration serum metabolites. Future studies, for example using absolute quantification of targeted metabolites, should provide additional information about the role of matrix effects. Our data indicate that biomarkers in ISF derive mostly from plasma, but there are also biomarkers specific to skin, many of which probably result from metabolic processes in the tissue and may be influenced by matrix effects.

Using a targeted approach to detect clinically valuable biomarkers, we found that most biomarkers detected in plasma were also in ISF, further supporting the idea that ISF may be a substitute for blood for diagnostic tests. Estimated concentrations of identified metabolites showed that diverse biomarkers were measurable in ISF at concentrations comparable to

plasma. These measurements were limited by the very small ISF sample volumes, leading to potential dilution errors and matrix effects resulting from differences in the physiology of the fluids. However, these results suggest that with collection of greater ISF sample volumes and methods validation, a broad spectrum of metabolites could be quantifiable using this method. Although this technique to sample ISF is currently more cumbersome than blood sampling by fingerstick, an advantage of ISF collection is that it is well suited to collection over time for biomarkers that may need a time-integrated measurement, more frequent monitoring, or continuous monitoring, since ISF does not clot.

Biomarkers found predominantly in ISF and not in blood include nucleosides such as cytidine and CMP (cancer biomarkers), 3-methyladenine (biomarker of DNA damage) and inosine (cardiac biomarker and neuroprotective agent for possible treatment of Parkinson's disease and multiple sclerosis). Several dermatologically relevant biomarkers like sphingosine (structural component of skin with signaling functionality), diethanolamine (carcinogen found in skin products) and vitamins D2 and E were also predominately detected in ISF. Additionally, exogenous molecules probably from environmental sources were found, like trans-cyclohexane-1,2-diol and methyl jasmonate.

We also compared biomarkers in ISF and SBF. Although most features were common to both biofluids, several were unique to ISF or SBF, probably due to differences in sampling methods. For example, corticosterone and 11-deoxycortisol (biomarkers associated with inflammation) were found only in SBF, which may represent a response to tissue damage during suction blister generation. In contrast, a derivative of leukotriene B4 (biomarker for vasodilation) was found in ISF samples, possibly because MN application can cause mild erythema. Fluid collected from the skin by other methods, such as microdialysis or open-flow microperfusion might show additional differences.

Several biomarkers with concentrations markedly elevated in ISF vs. plasma in the current study have been previously reported to be elevated in skin and sweat, suggesting that these values reflect true biological variation. For example, Stegink et al. (30) found that concentrations of the amino acids taurine, aspartate, threonine, serine, glycine, alanine, valine, leucine, tyrosine, phenylalanine, tryptophan, lysine, histidine, and ornithine (all higher in ISF in the current study) were higher in heel skin puncture vs. venous blood due to high levels on the skin surface, and Sakharov et al. (61) found that lactic acid (higher in ISF in the current study) was 10-fold higher in sweat vs. capillary blood. However, biomarker concentrations in ISF and SBF measured with this method need to be further validated using a matrix-matched reference standard.

Analysis and interpretation of the composition of a swab wiping of the skin surface is complicated. Biomarkers found on a swab rubbed against the skin with no MN treatment could be from the external environment and/or from the body. If from the external environment, the biomarker is not necessarily an artifact, since it is possible that the exogenous biomarker was absorbed into the skin and is truly found in ISF too. If from the body, the biomarker content of ISF collected from the skin surface could represent the true content in ISF, or could also represent a contribution from the biomarker previously secreted onto the skin surface by natural processes. Also, the effect of vacuum on possible

contamination with biomarkers from hair follicles and sweat glands onto the skin surface was not determined in this study and might play a role.

Targeted studies in human participants allowing absolute quantification of biomarker concentrations showed that pharmacokinetics of caffeine (used as a model biomarker in healthy adults) and pharmacodynamics of glucose (in diabetic children and young adults administered insulin after a standard meal) in ISF generally matched plasma, probably because small, hydrophilic molecules like caffeine and glucose rapidly equilibrate between blood and ISF across capillary walls (62). Previous studies in rats have similarly shown that glucose, vancomycin and rhodamine 6G have ISF kinetics similar to serum (48, 53, 54). This indicates the possibility of using ISF to continuously monitor biomarkers currently monitored in plasma, such as glucose, lactate, and urea, without indwelling, subcutaneous probes, and to perform continuous therapeutic drug monitoring of drugs with narrow therapeutic index, like vancomycin, warfarin and digoxin (63). Further optimization and research on the pharmacodynamics of biomarkers in skin is needed, in some cases with greater temporal resolution, to validate this approach to make clinical assessments based on biomarker concentrations measured in dermal ISF using this technique.

It is worth noting that ISF collected in this study is expected to contain only free (i.e., unbound) molecules similar to other ISF collection methods used for pharmacokinetic analysis (e.g., microdialysis, open-flow microperfusion), as opposed to collecting total (i.e., bound and unbound) molecules as via biopsy (64). Both molecules in the targeted-analysis studies are small, hydrophilic compounds that should easily traverse blood capillary walls. It is important in the future to carry out similar targeted analysis for hydrophobic and larger molecules that may bind to constituents of blood or may have difficulty crossing capillary walls, as seen in our previous studies in rats, where concentrations of the hydrophobic dye, rhodamine 6G (65), and anti-poliovirus antibodies (54), were present in ISF at concentrations lower than in serum. Kinetic analysis might also be affected by the use of vacuum, which may increase leakage from microcapillaries into ISF.

Device development required optimization to prevent ISF contamination with blood from broken capillaries. We noted that blood only appeared under vacuum, perhaps because MNs make very small incisions in capillaries that can self-seal, but vacuum forces them open. We found that using very short MNs (250 μm) and slowly ramping up vacuum after MN application could avoid bleeding and collect clean ISF samples. Future studies will be needed to determine if trace amounts of blood not found by visual observation might be present in ISF samples. Additional optimization work will be needed to reduce the variability of ISF collected from different study participants and at different time points.

ISF collection using MNs was well tolerated, with mild, transient erythema and reports of brief, minor pain similar to fingerstick. We believe that most pain came from sharp edges on the MN array backing, as opposed to the MNs themselves; this problem can be fixed with minor design modification. In support of this assertion, prior studies using much larger arrays of longer MNs have been reported painless (19, 66).

Intra-subject and inter-subject variability was observed in the volume of ISF collected. Better process controls and understanding of ISF fluid mechanics are needed to make the volume of ISF collected more reproducible. Further validation of methods used to calculate the volume of ISF collected (e.g., based on sodium concentration) would further improve accuracy of the biomarker measurements. Because this study included data from a limited number of human participants, corroboration and analysis of findings in larger populations are needed. Biomarker measurements in this study relied on LC-MS data only, and should be followed up with biomarker-specific assays to better quantify biomarker concentrations in ISF. Since this analysis is not based on absolute biomarker concentrations, biomarkers found to be common to two or more fluids may be present in these fluids at significantly different concentrations.

Future studies using this method should address analysis of ISF for a broader range of compounds, such as proteins; analysis of skin-site related differences in ISF composition since this study only looked at ISF collected on the forearm; further determination of the importance of biomarkers found in ISF and their relevance to human physiology; improvements in the reliability of ISF collection and methods to determine ISF volume collected; and device improvements that minimize pain. Moreover, we compared biofluid composition using samples obtained only included healthy participants and diabetic youth. Future research is needed to assess differences in ISF biomarkers among healthy populations and those with medical conditions.

In conclusion, progress in studying ISF as a source of biomarkers for diagnostic assays, dermatological drug pharmacology, tissue physiology and other applications has been limited by lack of simple, minimally invasive methods to collect ISF. In this study, we developed a method to sample ISF from skin using a MN-based device that was well-tolerated, minimally invasive, and relatively rapid to perform. Microliter quantities of ISF were collected, but there was variability in ISF volume that needs improvement by further process optimization. ISF sampled from human participants and analyzed for metabolites by LC-MS was found to have most molecular features in common with plasma and/or SBF, but some features were unique to ISF, including biomarkers of medical relevance. The pharmacokinetics of a model compound, caffeine, and the pharmacodynamics of glucose in ISF generally matched plasma in human participants. These findings suggest that ISF can be a source of valuable biomarkers as a non-clotting alternative to blood and a source of biomarkers unique to ISF for dermal and systemic physiology. Sampling ISF from skin using a MN patch has the potential for widespread use in research for biomarker discovery and drug development, as well as for possible future translation in the clinic for biomarker monitoring.

Methods

Study design

The primary goal of this study was to enable research and translation of ISF as a source of biomarkers. We therefore designed studies to (i) develop a method to sample ISF from skin of human participants, (ii) assess safety and acceptability of the method, (iii) characterize the breadth and possible clinical value of biomarkers found in ISF by metabolomic analysis

using LC-MS and (iv) assess the clinical utility of this technique by studying the pharmacokinetic relationship between a model biomarker concentration in ISF compared to blood and the pharmacodynamics of glucose concentrations in ISF and blood of type 1 diabetic children and young adults. Histopathological analysis of randomized hairless rat skin samples was conducted by a licensed dermatopathologist blinded to the experimental conditions (with or without MN and vacuum application).

Optimization of ISF collection methods using MNs was studied in five healthy adult volunteers (See Supplemental Materials and Methods). The endpoints were (i) amount of ISF collected and (ii) incidence or amount of bleeding. Each experimental condition was tested once in each subject. No outliers were excluded from the data. The study was not blinded. All procedures were approved by the Georgia Institute of Technology Institutional Review Board (IRB) and written consent was obtained from all subjects before the study. The study was not powered for statistical significance.

Metabolomic profiles of ISF, SBF, blood samples and skin swabs were obtained from 21 healthy adult volunteers. Metabolomic data from one subject was discarded because peak intensity was below that of water blank. Study samples provided for mass spectrometry analysis (conducted using 3 replicates per sample) were deidentified, randomized and blinded to the investigator running the analysis. Study endpoints were (i) prevalence of biomarkers in each fluid sample and (ii) differences in prevalence of biomarkers between fluid samples. All procedures were approved by the Georgia Institute of Technology IRB and written consent was obtained from all subjects before the study. The study was not powered for statistical significance.

Pharmacokinetics of caffeine, used as a model biomarker, was studied in nine healthy adult volunteers. Three volunteers returned for an additional visit for control experiments. Endpoints were (i) caffeine concentration in plasma and ISF over 8 h and (ii) volume of ISF collected. No outliers were excluded from the data. The study was not blinded. This study was approved by the Georgia Institute of Technology IRB. Recruitment for the caffeine study was based on a power analysis showing that with two independent study groups (caffeinated and non-caffeinated, $\alpha=0.05$, $\beta=0.8$, and enrollment ratio 3:1) statistical power could be achieved by enrolling 9 participants in Group 1 and 3 participants in Group 2. To facilitate statistical analysis, we determined that the concentration of caffeine in ISF and blood was normally distributed, as determined by the D'Agostino-Pearson normality test ($\alpha=0.05$, table S11).

Comparison of glucose concentrations in ISF and plasma was studied in fifteen type 1 diabetic children and young adults. Endpoints were (i) glucose concentrations in plasma and ISF over 3 h and (ii) volume of ISF collected. At the beginning of each study, participants were given a standard meal and a subcutaneous injection of insulin at a dose suitable for each participant's physiology. No outliers were excluded from the data, but ISF volume cut-offs were used to analyze subsets of the data. The study was not blinded. All procedures were approved by the Emory University and Georgia Institute of Technology IRBs and written consent was obtained from all subjects before the study. The study was not powered for statistical significance.

In the metabolomics and pharmacokinetics/pharmacodynamics studies, safety and acceptability of ISF collection were studied as well. Endpoints were (i) skin reaction determined by visual examination and palpation by study investigators and (ii) pain and other sensations reported by study participants. No outliers were excluded from the data. The study was intentionally not blinded to the study participants, because acceptability is based on the complete experience, which includes visual information.

Microneedle patch fabrication—MN patches were designed in Solidworks 2016 software (Solidworks) and fabricated from grade 316 stainless steel as five-needle planar arrays (Tech-Etch) by photo etching. MN length varied from 250 μm to 650 μm , with a cross-sectional area of 200 μm by 25 μm at the base and a sharp tapered tip of 10 μm diameter. MN patches were disinfected by washing with sterile 70% isopropyl alcohol (VWR) in a class II BSL hood (Thermo Fisher Scientific), packaged into self-sealing sterilization pouches (Crosstex International) and sterilized using an ethylene oxide sterilization cycle (AN74i Anprolene Gas Sterilizer, Andersen Products) that was validated using a product immersion method (WuXi AppTec). For the study in diabetic children, MN patches were manufactured at the Global Center for Medical Innovation (Atlanta, GA) and sterilized by a validated ethylene oxide sterilization cycle (Anderson Scientific).

ISF sampling using microneedle patches—ISF sampling through skin using MN patches was a two-step process: MN patch application to create micropores in the skin followed by application of vacuum to draw out ISF through the micropores.

Microneedle patch application: The site of MN patch application on the participant's forearm was disinfected using an alcohol swab (BD Alcohol Swab, BD), and an area of $\sim 50 \text{ mm}^2$ was marked with a pen. The investigator inserted a patch comprising a five-MN planar array at the site and then removed it immediately. This process was rapidly repeated 20 times per site to create an array of 100 micropores at each site (Movie S1).

Vacuum application: Vacuum was applied using a Negative Pressure Cutaneous Suction System (NP-2, Electronic Diversities). The vacuum chamber was aligned with skin sites that received MN treatment. Each chamber had a bottom plate with up to five 8-mm diameter orifices through which vacuum contacted the skin. Vacuum as low as -50 kPa (gauge) was applied for up to 20 min. In the optimized protocol, vacuum was slowly ramped down to -50 kPa over the course of $\sim 3 \text{ min}$. After stopping the vacuum after 20 min and removing the orifice plate, clear fluid on the skin surface was collected by rubbing the skin surface with a piece of sterile medical gauze (Ultrapure non-woven sponges, CrossTex International) wetted with 5–10 μL USP-grade sterile water for 30 s. This procedure helped collect extracted biomarkers from the skin because ISF may have evaporated during the collection process. The gauze was stored in a low protein-binding tube (Eppendorf North America) prior to placing in a -80°C freezer. To elute the sampled ISF biomarkers, the gauze was centrifuged along with 500 μL of sterile water at 4000 rpm for 30 min.

Blood collection by venipuncture—Venous blood ($\sim 5 \text{ mL}$) was collected from the forearm by venipuncture or via an intravenous catheter, collected into K3 EDTA tubes (BD Vacutainer Blood Collection Tube) and spun down at 1,400 rcf for 15 min (Eppendorf

centrifuge 5702 RH, Eppendorf AG) to separate the plasma, which was collected in Protein lo-bind tubes (Eppendorf Lo-bind). Capillary blood samples were collected by lancet puncture on the fingertip (Unistik 2 Normal, Owen Mumford) and collected into heparin mini collection tubes (MiniCollect Lithium Heparin with Gel Separator, Gernier Bio One North America). The tubes were spun down at 1,400 rcf for 15 min (Eppendorf centrifuge 5702 RH) to separate the plasma, which was collected in Protein lo-bind tubes. All plasma samples were stored at -80°C until analysis.

Suction blister fluid collection from suction blisters—SBF was collected by the method developed by Kiistala (15). Suction blisters were created on the thigh of each participant as a site easily accessible when wearing shorts and one that can be discretely covered for cosmetic reasons until suction blisters have fully healed. The skin site was first thoroughly disinfected with an alcohol swab. Suction was then applied using a Negative Pressure Cutaneous Suction System (NPV-2, Electronic Diversities). Sterile orifice plates with 3 holes (8 mm diameter each) along with the suction cup were firmly attached to the skin using straps. Suction at -50 to -70 kPa (gauge) was applied at 40°C for ~ 45 min until blister formation was complete. Fluid from intact and hemoglobin-free blisters (~ 50 μL per blister) was collected using a Micro-Fine syringe (BD Biosciences) and stored in Protein lo-bind Eppendorf tubes at -80°C .

Skin surface swab—Sterile medical gauze wetted with sterile USP-grade water was rubbed against the skin for 30 s and stored in Protein lo-bind Eppendorf tubes at -80°C .

Caffeine pharmacokinetics study—Nine healthy adults (table S8) were recruited for the study and provided informed consent to participate. Participation was open to any healthy adult. Exclusion criteria included serious dermatological conditions, pregnancy, immunodeficiency, recent blood donation and anemia. Participants were told to refrain from consuming caffeine for 36 hours before the study. Each participant drank a 12 ounce can of Diet Coke containing 43 mg of caffeine (Coca Cola) within 5 minutes. Three of the participants were studied a second time on a different day following the same protocol, except they drank caffeine-free Diet Coke instead of the caffeinated Diet Coke. ISF and blood samples were collected before and 0.5, 1, 2, 4 and 8 hours afterward drinking the Diet Coke. ISF and plasma caffeine concentrations were determined as described below.

Glucose pharmacodynamics study—Fifteen healthy children and young adults with type 1 diabetes (11 – 25 years old) were recruited for the study (See table S9 for demographics). For subjects <18 years old, the child's guardian provided informed consent to participate, and the subject provided an informed assent. If the subject was ≥ 18 years old, the subject provided informed consent. Inclusion criteria included (i) ≥ 7 years old, (ii) type 1 diabetes diagnosed for at least 2 years and (iii) good glucose control ($\text{A1C} < 8.5\%$). Exclusion criteria included (i) pregnancy and (ii) taking high-dose glucocorticoid therapy. Participants were given a standard meal containing 60 – 75 grams of carbohydrates and, immediately after the meal, administered a dose of lispro insulin (Humalog, Eli Lilly) appropriate for the meal consumed and the participant's physiology, as determined by a pediatric endocrinologist in consultation with the participant and/or guardian. ISF and blood

samples were collected before and 1, 2 and 3 hours after eating the meal. ISF and plasma glucose concentrations were determined as described below. Anxiety (before ISF and blood collection) and pain (after ISF and blood collection) of subjects was assessed by visual analog pain scale.

Analytical techniques

Determination of blood volume: Collected blood volume was measured by determining hemoglobin content in blood samples using a Triton / NaOH-based method (Hemoglobin Assay Kit, Sigma-Aldrich). Hemoglobin content in a blood sample was normalized against hemoglobin content in the capillary blood of the same participant to obtain the amount of blood in each sample.

Determination of ISF volume: Collected ISF volume was measured by determining sodium ion concentration in the collected fluid. Sodium ion concentration was determined using a sodium ion-selective electrode (perfectION comb NA, Mettler Toledo). The sodium ion content measured in the samples was normalized against a standard sodium ion concentration in ISF of 135 mmol/L to determine ISF volume. Measurement of sodium in the surface swabs used as a ‘negative’ control showed that the amount of sodium was below the detection limit of the analyzer and was therefore effectively taken as zero.

High-resolution metabolomics: Body fluids (ISF, SBF and plasma) were profiled using untargeted high-resolution metabolomics (HRM) with dual column/polarity liquid chromatography. Body fluid samples were diluted from 10 μ L to 50 μ L with distilled water, and treated with 100 μ L of acetonitrile containing a mixture of 11 stable isotope standards. Samples were vortexed and allowed to equilibrate before proteins were precipitated by centrifuge for 10 minutes at 14,100 rcf maintained at 4°C. Samples were analyzed using hydrophilic interaction chromatography (HILIC; XBridge BEH Amide XP, 2.1 mm x 50 mm x 2.5 μ m particle size, Waters) in positive electrospray ionization mode, which better captured polar and semi-polar metabolites, and using reverse-phase C18 liquid chromatography (stainless steel column, 2.1 mm x 50 mm x 3 μ m particle size, Higgins) in negative-ion mode, which better captured fatty acids and other nonpolar metabolites. The dual chromatography setup interfaced to a high-resolution Fourier transform mass spectrometer (Q-Exactive HF, Thermo Scientific).

For each mode, analyses were performed with three technical replicates with an injection volume of 10 μ L and mass-to-charge ratio (m/z) scan range of 85 to 1275. Body fluid types were analyzed in separate batches, with samples randomized within each fluid and distilled water blanks and pooled reference plasma (Q-Standard) samples analyzed prior to and following each batch to enable quality control, as described previously (67). Data extraction was performed using apLCMS (68) and xMSanalyzer (69) as m/z features, with an m/z feature defined by m/z , retention time, and ion abundance. Triplicates were averaged prior to data analysis. A feature was defined as “present” in a sample if the ion intensity in the sample was greater than two times the mean ion intensity of that feature in the water blank samples. Data were filtered to remove features that were not present in 50% of samples in at least one body fluid.

Metabolite identification: Clinically-relevant biomarkers were identified by comparing detected peak accurate mass m/z and retention time to a library of confirmed authentic reference standards that were analyzed under identical assay conditions (67) using an m/z threshold of 10 ppm and retention time difference of 30 s. Metabolites unique to ISF and/or SBF were also identified using a dataset-wide deconvolution algorithm that leverages a combination of adduct grouping, isotope similarity, mass defect filtering, correlation and retention time clustering to reduce false positive annotations and Kyoto Encyclopedia of Genes and Genomes (KEGG) (70) database matching (± 10 ppm). For the latter, high-confidence matches (metabolites with two or more correlated adducts and/or isotopes with similar retention times) were curated to remove unlikely peak groupings and/or biologically-implausible compounds. The presence or absence of a metabolite was evaluated by examining the base peak in the feature grouping. If a metabolite was identified using both C18 and HILIC, results were reported for the chromatography method with the higher number of detectable values for the corresponding metabolite across all study samples. Metabolite identification confidence levels were classified according to the Metabolomics Standards Initiative (71), in which clinically relevant biomarkers matching the standards library were classified as level 1 (“confidently identified compounds”), while annotated compounds based on mass spectral clusters were classified as level 2 (“putatively annotated compounds”).

Reference standardization: Absolute concentrations of metabolites were quantified by reference standardization for the 65 metabolites detected in the study samples from the Mass Spectrometry Metabolite Library of Standards (MSMLS; IROA Technologies, Sea Girt, NJ, USA) that were also detected in the lab’s reference pooled plasma sample (28, 29). Using this approach, metabolite concentrations previously determined in pooled plasma (referred to as Q-Std3) by methods of addition or comparison to NIST standard reference material 1950 (Metabolites in Frozen Human Plasma) (29, 72–74) were used as a reference standard for each analyte. ISF, plasma, and SBF concentrations were calculated using single point calibration by multiplying the analyte response factor (calculated as the ratio between the known concentration of the compound being quantified and ion intensity in Q-Std3) and metabolite intensity detected in each study sample.

Determination of caffeine concentration: Caffeine concentration in plasma was measured using a commercial enzyme-linked immunoassay (ELISA) kit (Abraxis). Because ISF at least partially evaporated before analysis, the amount of caffeine in the collected ISF was determined by ELISA and divided by the volume of ISF collected to determine caffeine concentration in the ISF. For each subject, the background signal of the caffeine assay from the skin surface, detected using the surface swab, was subtracted to get the amount of caffeine in the extracted ISF.

Calculation of pharmacokinetic parameters: C_{\max} was the highest caffeine concentration measured in ISF/plasma from each participant. t_{\max} was the time at which C_{\max} was measured. Area under the curve, $AUC_{(0-8h)}$, was calculated using the linear trapezoidal rule. To estimate half-life, $t_{1/2}$, an elimination rate constant (k_e) was obtained as the slope of the elimination curve on a semilog plot (fig. S18), and then $t_{1/2}$ was calculated as $t_{1/2} = \ln(2)/k_e$.

To estimate clearance (CL), the apparent volume of distribution (V_D) was multiplied by k_e . V_D was calculated as D/C_0 where D is the dose of caffeine (43 mg) and C_0 is the intercept of the elimination curve on the y axis.

Determination of glucose concentration: Glucose concentration in plasma was determined by a glucose analyzer (Yellow Springs Instrument). Glucose content in collected ISF samples was measured (Amplex Red Glucose Assay Kit, Thermo Fisher Scientific) and divided by the volume of ISF collected to determine glucose concentration in ISF (see Supplementary Materials and Methods). Glucose concentration in ISF and plasma were compared by plotting on a Clarke error grid, considering samples with ISF volumes 0.60 μ L (21 of 58 samples) and 0.25 μ L (34 of 58 samples).

Statistical analysis

All statistical analysis was conducted using Graphpad Prism 7 Software (GraphPad Software). Statistical differences with two test groups were analyzed using Student's t-test. For groups of three or more, one-way ANOVA test was used to establish statistical difference. P-value of <0.05 was considered statistically significant.

Supplementary Material

Refer to Web version on PubMed Central for supplementary material.

Acknowledgements:

The authors thank D. Bondy for administrative support; S. Henry and D. McAllister for helping with study design; C. Ma for help analyzing samples using LC-MS; and B. Pollack for analyzing skin histopathological samples. **Funding:** This work was supported in part by the U.S. National Institutes of Health (U2CES026560, P30ES020953, R01ES023485, P30ES019776, S10OD018006) and Children's Healthcare of Atlanta. PPS is currently a clinical research scientist at Apple. MMN is currently an assistant professor of environmental medicine & public health at the Icahn School of Medicine at Mount Sinai. DIW is currently an assistant professor of environmental medicine & public health at the Icahn School of Medicine at Mount Sinai. GWM is currently a professor of environmental health sciences at Columbia University. MRP is also a professor of biomedical engineering at Georgia Tech and Emory University and is an adjunct professor of chemical and biomolecular engineering at the Korea Advanced Institute of Science & Technology.

Data and materials availability:

All data associated with this study are present in the paper or the Supplementary Materials.

References:

1. Downing GJ, in *Pharmaceutical Sciences Encyclopedia*. (John Wiley & Sons, Inc, 2010).
2. Heikenfeld J, Jajack A, Feldman B, Granger SW, Gaitonde S, Begtrup G, Katchman BA, Accessing analytes in biofluids for peripheral biochemical monitoring. *Nature biotechnology* 37, 407–419 (2019); published online EpubApr (10.1038/s41587-019-0040-3).
3. Deacon B, Abramowitz J, Fear of needles and vasovagal reactions among phlebotomy patients. *Journal of Anxiety Disorders* 20, 946–960 (2006); published online Epub2006/01/01/ (10.1016/j.janxdis.2006.01.004). [PubMed: 16460906]
4. Fischbach FT, Dinning MB, *A manual of laboratory and diagnostic tests*. (Wolters Kluwer Health, ed. 8th edition, 2009), pp. 1283.

5. Fogh-Andersen N, Altura BM, Altura BT, Siggaard-Andersen O, Composition of interstitial fluid. *Clinical chemistry* 41, 1522–1525 (1995); published online EpubOct ([PubMed: 7586528]
6. Muller AC, Breitwieser FP, Fischer H, Schuster C, Brandt O, Colinge J, Superti-Furga G, Stingl G, Elbe-Burger A, Bennett KL, A comparative proteomic study of human skin suction blister fluid from healthy individuals using immunodepletion and iTRAQ labeling. *J Proteome Res* 11, 3715–3727 (2012); published online EpubJul 6 (10.1021/pr3002035). [PubMed: 22578099]
7. Tran BQ, Miller PR, Taylor RM, Boyd G, Mach PM, Rosenzweig CN, Baca JT, Polsky R, Glaros T, Proteomic Characterization of Dermal Interstitial Fluid Extracted Using a Novel Microneedle-Assisted Technique. *Journal of Proteome Research* 17, 479–485 (2018); published online Epub2018/01/05 (10.1021/acs.jproteome.7b00642). [PubMed: 29172549]
8. Miller PR, Taylor RM, Tran BQ, Boyd G, Glaros T, Chavez VH, Krishnakumar R, Sinha A, Poorey K, Williams KP, Extraction and biomolecular analysis of dermal interstitial fluid collected with hollow microneedles. *Communications biology* 1, 173 (2018). [PubMed: 30374463]
9. Kool J, Reubsaet L, Wesseldijk F, Maravilha RT, Pinkse MW, D’Santos CS, van Hilten JJ, Zijlstra FJ, Heck AJ, Suction blister fluid as potential body fluid for biomarker proteins. *Proteomics* 7, 3638–3650 (2007); published online EpubOct (10.1002/pmic.200600938). [PubMed: 17890648]
10. Renard E, Implantable continuous glucose sensors. *Current diabetes reviews* 4, 169–174 (2008). [PubMed: 18690897]
11. Herkenne C, Alberti I, Naik A, Kalia YN, Mathy F-X, Pr eat V, Guy RH, In vivo methods for the assessment of topical drug bioavailability. *Pharmaceutical Research* 25, 87 (2008). [PubMed: 17985216]
12. Wiig H, Tenstad O, Iversen PO, Kalluri R, Bjerkvig R, Interstitial fluid: the overlooked component of the tumor microenvironment? *Fibrogenesis & tissue repair* 3, 12 (2010)10.1186/1755-1536-3-12). [PubMed: 20653943]
13. Pierre Agache PH, Measuring The Skin. Philipp M, Ed., (Springer-Verlag Berlin Heidelberg New York, 2004), pp. 784.
14. Haslene-Hox H, Oveland E, Berg KC, Kolmannskog O, Woie K, Salvesen HB, Tenstad O, Wiig H, A new method for isolation of interstitial fluid from human solid tumors applied to proteomic analysis of ovarian carcinoma tissue. *PLoS One* 6, e19217 (2011). [PubMed: 21541282]
15. Kiistala U, Suction blister device for separation of viable epidermis from dermis. *The Journal of Investigative Dermatology* 15, 129–137 (1968).
16. Schmidt S, Banks R, Kumar V, Rand KH, Derendorf H, Clinical microdialysis in skin and soft tissues: an update. *The Journal of Clinical Pharmacology* 48, 351–364 (2008). [PubMed: 18285620]
17. Bodenlenz M, Tiffner KI, Raml R, Augustin T, Dragatin C, Birngruber T, Schimek D, Schwagerle G, Pieber TR, Raney SG, Kanfer I, Sinner F, Open flow microperfusion as a dermal pharmacokinetic approach to evaluate topical bioequivalence. *Clinical Pharmacokinetics* 56, 91–98 (2017); published online EpubJan (10.1007/s40262-016-0442-z). [PubMed: 27539717]
18. Sieg A, Guy RH, Bego na Delgado-Charro M, Electroosmosis in Transdermal Iontophoresis: Implications for Noninvasive and Calibration-Free Glucose Monitoring. *Biophysical Journal* 87, 3344–3350 (2004); published online Epub11// (10.1529/biophysj.104.044792). [PubMed: 15339817]
19. Norman JJ, Arya JM, McClain MA, Frew PM, Meltzer MI, Prausnitz MR, Microneedle patches: usability and acceptability for self-vaccination against influenza. *Vaccine* 32, 1856–1862 (2014); published online EpubApr 1 (10.1016/j.vaccine.2014.01.076). [PubMed: 24530146]
20. Caffarel-Salvador E, Brady AJ, Eltayib E, Meng T, Alonso-Vicente A, Gonzalez-Vazquez P, Torrisi BM, Vicente-Perez EM, Mooney K, Jones DS, Bell SEJ, McCoy CP, McCarthy HO, McElnay JC, Donnelly RF, Hydrogel-forming microneedle arrays allow detection of drugs and glucose *in vivo*: Potential for use in diagnosis and therapeutic drug monitoring. *PLoS ONE* 10, e0145644 (2016)10.1371/journal.pone.0145644).
21. Ranamukhaarachchi SA, Padeste C, D ubner M, H afeli UO, Stoeber B, Cadarso VJ, Integrated hollow microneedle-optofluidic biosensor for therapeutic drug monitoring in sub-nanoliter volumes. *Scientific Reports* 6, 29075 (2016); published online Epub07/06/online (10.1038/srep29075). [PubMed: 27380889]

22. Banga AK, Transdermal and intradermal delivery of therapeutic agents: Application of physical technologies. (Taylor and Francis Group LLC, Boca Raton, FL, 2011), pp. 282.
23. Prausnitz MR, Engineering microneedle patches for vaccination and drug delivery to skin. *Annual Review of Chemical and Biomolecular Engineering* 8, 177–200 (2017).
24. Junge T, Blood clotting mechanism. *Surgical Technologist* 38, 12 (2006).
25. Kiiistala U, Mustakallio KK, Dermo-Epidermal Separation with Suction: Electron Microscopic and Histochemical Study of Initial Events of Blistering on Human Skin*. *Journal of Investigative Dermatology* 48, 466–477 (1967); published online Epub1967/05/01/ (10.1038/jid.1967.72).
26. Niedzwiecki MM, Samant P, Walker DI, Tran V, Jones DP, Prausnitz MR, Miller GW, Human Suction Blister Fluid Composition Determined Using High-Resolution Metabolomics. *Analytical Chemistry* 90, 3786–3792 (2018); published online Epub2018/03/20 (10.1021/acs.analchem.7b04073). [PubMed: 29425024]
27. Kinn PM, Holdren GO, Westermeyer BA, Abuissa M, Fischer CL, Fairley JA, Brogden KA, Brogden NK, Age-dependent variation in cytokines, chemokines, and biologic analytes rinsed from the surface of healthy human skin. *Scientific Reports* 5, 10472 (2015); published online Epub06/02 [PubMed: 26035055]
28. Go YM, Walker DI, Liang Y, Uppal K, Soltow QA, Tran V, Strobel F, Quyyumi AA, Ziegler TR, Pennell KD, Miller GW, Jones DP, Reference Standardization for Mass Spectrometry and High-resolution Metabolomics Applications to Exposome Research. *Toxicol Sci* 148, 531–543 (2015); published online EpubDec (10.1093/toxsci/kfv198). [PubMed: 26358001]
29. Liu KH, Nellis M, Uppal K, Ma C, Tran V, Liang Y, Walker DI, Jones DP, Reference Standardization for Quantification and Harmonization of Large-Scale Metabolomics. *Anal Chem*, (2020); published online EpubJun 15 (10.1021/acs.analchem.0c00338).
30. Stegink LD, Filer LJ, Baker GL, Effect of sampling site on plasma amino acid concentrations of infants: effect of skin amino acids. *Am J Clin Nutr* 36, 917–925 (1982); published online EpubNov (10.1093/ajcn/36.5.917). [PubMed: 7137076]
31. Terao M, Katayama I, Local cortisol/corticosterone activation in skin physiology and pathology. *Journal of Dermatological Science* 84, 11–16 (2016)10.1016/j.jdermsci.2016.06.014). [PubMed: 27431412]
32. Garza C, “Pharmacology of Caffeine,” Caffeine for the Sustainment of Mental Task Performance: Formulations for Military Operations. (Committee on Military Nutrition Research, Food and Nutrition Board, National Academies Press (US), Washington D.C., 2001).
33. Liguori A, Hughes JR, Grass JA, Absorption and subjective effects of caffeine from coffee, cola and capsules. *Pharmacology Biochemistry and Behavior* 58, 721–726 (1997).
34. Jacobson AF, Cerqueira MD, Raisys V, Shattu S, Serum caffeine levels after 24 hours of caffeine abstinence: observations on clinical patients undergoing myocardial perfusion imaging with dipyridamole or adenosine. *European Journal of Nuclear Medicine and Molecular Imaging* 21, 23–26 (1994).
35. Collomp K, Anselme F, Audran M, Gay JP, Chanal JL, Prefaut C, Effects of moderate exercise on the pharmacokinetics of caffeine. *European Journal of Clinical Pharmacology* 40, 279–282 (1991); published online EpubMarch 01 (10.1007/bf00315209). [PubMed: 2060565]
36. Stout PJ, Racchini JR, Hilgers ME, A novel approach to mitigating the physiological lag between blood and interstitial fluid glucose measurements. *Diabetes Technol Ther* 6, 635–644 (2004); published online EpubOct (10.1089/dia.2004.6.635). [PubMed: 15628817]
37. Kulcu E, Tamada JA, Reach G, Potts RO, Lesho MJ, Physiological differences between interstitial glucose and blood glucose measured in human subjects. *Diabetes care* 26, 2405–2409 (2003). [PubMed: 12882870]
38. Guo J, Whittemore R, He GP, The relationship between diabetes self-management and metabolic control in youth with type 1 diabetes: an integrative review. *Journal of advanced nursing* 67, 2294–2310 (2011); published online EpubNov (10.1111/j.1365-2648.2011.05697.x). [PubMed: 21615460]
39. Sieg A, Guy RH, Delgado-Charro MB, Noninvasive glucose monitoring by reverse iontophoresis in vivo: application of the internal standard concept. *Clinical chemistry* 50, 1383–1390 (2004); published online EpubAug (10.1373/clinchem.2004.032862). [PubMed: 15155544]

40. Hillier TA, Abbott RD, Barrett EJ, Hyponatremia: evaluating the correction factor for hyperglycemia. *The American journal of medicine* 106, 399–403 (1999). [PubMed: 10225241]
41. Tamada JA, Garg S, Jovanovic L, Pitzer KR, Fermi S, Potts RO, Noninvasive glucose monitoring: comprehensive clinical results. Cygnus Research Team. *Jama* 282, 1839–1844 (1999); published online EpubNov 17 ([PubMed: 10573275]
42. Schafflhuber M, Volpi N, Dahlmann A, Hilgers KF, Maccari F, Dietsch P, Wagner H, Luft FC, Eckardt KU, Titze J, Mobilization of osmotically inactive Na⁺ by growth and by dietary salt restriction in rats. *American journal of physiology. Renal physiology* 292, F1490–1500 (2007); published online EpubMay (10.1152/ajprenal.00300.2006). [PubMed: 17244896]
43. Hofmeister LH, Perisic S, Titze J, Tissue sodium storage: evidence for kidney-like extrarenal countercurrent systems? *Pflugers Archiv : European journal of physiology* 467, 551–558 (2015); published online EpubMar (10.1007/s00424-014-1685-x). [PubMed: 25600900]
44. Levick JR, Michel CC, Microvascular fluid exchange and the revised Starling principle. *Cardiovascular research* 87, 198–210 (2010); published online EpubJul 15 (10.1093/cvr/cvq062). [PubMed: 20200043]
45. Riemsma R, Corro Ramos I, Birnie R, Büyükkaramikli N, Armstrong N, Ryder S, Duffy S, Worthy G, Al M, Severens J, Kleijnen J, Integrated sensor-augmented pump therapy systems [the MiniMed® Paradigm™ Veo system and the Vibe™ and G4® PLATINUM CGM (continuous glucose monitoring) system] for managing blood glucose levels in type 1 diabetes: a systematic review and economic evaluation. *Health Technology Assessment (Winchester, England)* 20, 1–252 (2016)10.3310/hta20170).
46. Hammarlund-Udenaes M, Microdialysis as an Important Technique in Systems Pharmacology—a Historical and Methodological Review. *The AAPS Journal*, 1–10 (2017).
47. Miller PR, Skoog SA, Edwards TL, Wheeler DR, Xiao X, Brozik SM, Polsky R, Narayan RJ, Hollow microneedle-based sensor for multiplexed transdermal electrochemical sensing. *Journal of Visualized Experiments : JoVE*, 4067 (2012); published online Epub06/01 (10.3791/4067). [PubMed: 22688693]
48. Wang PM, Cornwell M, Prausnitz MR, Minimally invasive extraction of dermal interstitial fluid for glucose monitoring using microneedles. *Diabetes Technol Ther* 7, 131–141 (2005); published online EpubFeb (10.1089/dia.2005.7.131). [PubMed: 15738711]
49. Jina A, Tierney MJ, Tamada JA, McGill S, Desai S, Chua B, Chang A, Christiansen M, Design, development, and evaluation of a novel microneedle array-based continuous glucose monitor. *J Diabetes Sci Technol* 8, 483–487 (2014); published online EpubMay (10.1177/1932296814526191). [PubMed: 24876610]
50. Caffarel-Salvador E, Brady AJ, Eltayib E, Meng T, Alonso-Vicente A, Gonzalez-Vazquez P, Torrisi BM, Vicente-Perez EM, Mooney K, Jones DS, Bell SEJ, McCoy CP, McCarthy HO, McElnay JC, Donnelly RF, Hydrogel-forming microneedle arrays allow detection of drugs and glucose: Potential for use in diagnosis and therapeutic drug monitoring. *PLoS ONE* 10, e0145644 (2016)10.1371/journal.pone.0145644).
51. Mandal A, Boopathy AV, Lam LK, Moynihan KD, Welch ME, Bennett NR, Turvey ME, Thai N, Van JH, Love JC, Cell and fluid sampling microneedle patches for monitoring skin-resident immunity. *Science translational medicine* 10, eaar2227 (2018). [PubMed: 30429353]
52. Chang H, Zheng M, Yu X, Than A, Seeni RZ, Kang R, Tian J, Khanh DP, Liu L, Chen P, Xu C, A Swellable Microneedle Patch to Rapidly Extract Skin Interstitial Fluid for Timely Metabolic Analysis. *Advanced materials (Deerfield Beach, Fla.)* 29, (2017); published online EpubOct (10.1002/adma.201702243).
53. Kolluru C, Williams M, Chae J, Prausnitz MR, Recruitment and Collection of Dermal Interstitial Fluid Using a Microneedle Patch. *Advanced healthcare materials*, 1801262 (2019).
54. Kolluru C, Williams M, Yeh JS, Noel RK, Knaack J, Prausnitz MR, Monitoring drug pharmacokinetics and immunologic biomarkers in dermal interstitial fluid using a microneedle patch. *Biomedical Microdevices* 21, 14 (2019). [PubMed: 30725230]
55. Tran BQ, Miller PR, Taylor RM, Boyd G, Mach PM, Rosenzweig CN, Baca JT, Polsky R, Glaros T, Proteomic characterization of dermal interstitial fluid extracted using a novel microneedle-assisted technique. *Journal of proteome research* 17, 479–485 (2017). [PubMed: 29172549]

56. Taylor RM, Miller PR, Ebrahimi P, Polsky R, Baca JT, Minimally-invasive, microneedle-array extraction of interstitial fluid for comprehensive biomedical applications: transcriptomics, proteomics, metabolomics, exosome research, and biomarker identification. *Laboratory animals*, 0023677218758801 (2018).
57. Stout PJ, Peled N, Erickson BJ, Hilgers ME, Racchini JR, Hoegh TB, Comparison of glucose levels in dermal interstitial fluid and finger capillary blood. *Diabetes technology & therapeutics* 3, 81–90 (2001). [PubMed: 11469711]
58. Gebhart S, Faupel M, Fowler R, Kapsner C, Lincoln D, McGee V, Pasqua J, Steed L, Wangsness M, Xu F, Glucose sensing in transdermal body fluid collected under continuous vacuum pressure via micropores in the stratum corneum. *Diabetes technology & therapeutics* 5, 159–166 (2003). [PubMed: 12871605]
59. Venugopal M, Arya SK, Chornokur G, Bhansali S, A realtime and continuous assessment of cortisol in ISF using electrochemical impedance spectroscopy. *Sensors and Actuators A: Physical* 172, 154–160 (2011). [PubMed: 22163154]
60. Samant PP, Prausnitz MR, Mechanisms of sampling interstitial fluid from skin using a microneedle patch. *Proceedings of the National Academy of Sciences of the United States of America* 115, 4583–4588 (2018); published online EpubMay 1 (10.1073/pnas.1716772115). [PubMed: 29666252]
61. Sakharov DA, Shkurnikov MU, Vagin MY, Yashina EI, Karyakin AA, Tonevitsky AG, Relationship between lactate concentrations in active muscle sweat and whole blood. *Bull Exp Biol Med* 150, 83–85 (2010); published online EpubDec (10.1007/s10517-010-1075-0). [PubMed: 21161059]
62. Scuffi C, Interstitium Versus Blood Equilibrium in Glucose Concentration and its Impact on Subcutaneous Continuous Glucose Monitoring Systems. *Euro Endocrin* 10, 36–42 (2014).
63. Yu LX, Jiang W, Zhang X, Lionberger R, Makhlof F, Schuirmann DJ, Muldowney L, Chen ML, Davit B, Conner D, Woodcock J, Novel bioequivalence approach for narrow therapeutic index drugs. *Clinical pharmacology and therapeutics* 97, 286–291 (2015); published online EpubMar (10.1002/cpt.28). [PubMed: 25669762]
64. Kiang TK, Schmitt V, Ensom MH, Chua B, Häfeli UO, Therapeutic drug monitoring in interstitial fluid: a feasibility study using a comprehensive panel of drugs. *Journal of pharmaceutical sciences* 101, 4642–4652 (2012). [PubMed: 22941939]
65. Kolluru C, Gupta R, Jiang Q, Williams M, Gholami Derami H, Cao S, Noel RK, Singamaneni S, Prausnitz MR, Plasmonic Paper Microneedle Patch for On-Patch Detection of Molecules in Dermal Interstitial Fluid. *ACS sensors* 4, 1569–1576 (2019). [PubMed: 31070358]
66. Gill HS, Denson DD, Burris BA, Prausnitz MR, Effect of microneedle design on pain in human volunteers. *The Clinical journal of pain* 24, 585–594 (2008); published online EpubSep (10.1097/AJP.0b013e31816778f9). [PubMed: 18716497]
67. Go Y-M, Walker DI, Liang Y, Uppal K, Soltow QA, Tran V, Strobel F, Quyyumi AA, Ziegler TR, Pennell KD, Miller GW, Jones DP, Reference standardization for mass spectrometry and high-resolution metabolomics applications to exposome research. *Toxicological Sciences* 148, 531–543 (2015). [PubMed: 26358001]
68. Yu T, Park Y, Johnson JM, Jones DP, apLCMS—adaptive processing of high-resolution LC/MS data. *Bioinformatics* 25, 1930–1936 (2009); published online Epub05/04 [PubMed: 19414529]
69. Uppal K, Soltow QA, Strobel FH, Pittard WS, Gernert KM, Yu T, Jones DP, xMSAnalyzer: automated pipeline for improved feature detection and downstream analysis of large-scale, non-targeted metabolomics data. *BMC Bioinformatics* 14, 15 (2013); published online Epub2013/01/16 (10.1186/1471-2105-14-15). [PubMed: 23323971]
70. Kanehisa M, Goto S, Sato Y, Furumichi M, Tanabe M, KEGG for integration and interpretation of large-scale molecular data sets. *Nucleic Acids Research* 40, D109–D114 (2012); published online Epub11/10 [PubMed: 22080510]
71. Sumner LW, Amberg A, Barrett D, Beale MH, Beger R, Daykin CA, Fan TWM, Fiehn O, Goodacre R, Griffin JL, Hankemeier T, Hardy N, Harnly J, Higashi R, Kopka J, Lane AN, Lindon JC, Marriott P, Nicholls AW, Reily MD, Thaden JJ, Viant MR, Proposed minimum reporting standards for chemical analysis Chemical Analysis Working Group (CAWG) Metabolomics

- Standards Initiative (MSI). *Metabolomics* 3, 211–221 (2007)10.1007/s11306-007-0082-2). [PubMed: 24039616]
72. Simón-Manso Y, Lowenthal MS, Kilpatrick LE, Sampson ML, Telu KH, Rudnick PA, Mallard WG, Bearden DW, Schock TB, Tchekhovskoi DV, Blonder N, Yan X, Liang Y, Zheng Y, Wallace WE, Neta P, Phinney KW, Remaley AT, Stein SE, Metabolite profiling of a NIST Standard Reference Material for human plasma (SRM 1950): GC-MS, LC-MS, NMR, and clinical laboratory analyses, libraries, and web-based resources. *Anal Chem* 85, 11725–11731 (2013); published online EpubDec 17 (10.1021/ac402503m). [PubMed: 24147600]
73. Quehenberger O, Armando AM, Brown AH, Milne SB, Myers DS, Merrill AH, Bandyopadhyay S, Jones KN, Kelly S, Shaner RL, Sullards CM, Wang E, Murphy RC, Barkley RM, Leiker TJ, Raetz CR, Guan Z, Laird GM, Six DA, Russell DW, McDonald JG, Subramaniam S, Fahy E, Dennis EA, Lipidomics reveals a remarkable diversity of lipids in human plasma. *J Lipid Res* 51, 3299–3305 (2010); published online EpubNov (10.1194/jlr.M009449). [PubMed: 20671299]
74. Colas RA, Shinohara M, Dalli J, Chiang N, Serhan CN, Identification and signature profiles for pro-resolving and inflammatory lipid mediators in human tissue. *Am J Physiol Cell Physiol* 307, C39–54 (2014); published online EpubJul 1 (10.1152/ajpcell.00024.2014). [PubMed: 24696140]
75. Gibbs NK, Norval M, Urocanic Acid in the Skin: A Mixed Blessing? *Journal of Investigative Dermatology* 131, 14–17 (2011); published online Epub2011/01/01/ (10.1038/jid.2010.276).
76. Marescau B, De Deyn PP, Holvoet J, Possemiers I, Nagels G, Saxena V, Mahler C, Guanidino compounds in serum and urine of cirrhotic patients. *Metabolism: clinical and experimental* 44, 584–588 (1995); published online EpubMay ([PubMed: 7752905]
77. Chen L, Fan J, Li Y, Shi X, Ju D, Yan Q, Yan X, Han L, Zhu H, Modified Jiu Wei Qiang Huo decoction improves dysfunctional metabolomics in influenza A pneumonia-infected mice. *Biomedical chromatography : BMC* 28, 468–474 (2014); published online EpubApr (10.1002/bmc.3055). [PubMed: 24132661]
78. Jiang Q, Christen S, Shigenaga MK, Ames BN, gamma-tocopherol, the major form of vitamin E in the US diet, deserves more attention. *Am J Clin Nutr* 74, 714–722 (2001); published online EpubDec ([PubMed: 11722951]
79. Li J, Xiao LT, Zeng GM, Huang GH, Shen GL, Yu RQ, Amperometric immunosensor based on polypyrrole/poly(m-phenylenediamine) multilayer on glassy carbon electrode for cytokinin N6-(Delta2-isopentenyl) adenosine assay. *Analytical biochemistry* 321, 89–95 (2003); published online EpubOct 1 ([PubMed: 12963059]
80. Boudonck KJ, Mitchell MW, Németh L, Keresztes L, Nyska A, Shinar D, Rosenstock M, Discovery of metabolomics biomarkers for early detection of nephrotoxicity. *Toxicologic pathology* 37, 280–292 (2009). [PubMed: 19380839]
81. Kimura T, Yasuda K, Yamamoto R, Soga T, Rakugi H, Hayashi T, Isaka Y, Identification of biomarkers for development of end-stage kidney disease in chronic kidney disease by metabolomic profiling. *Scientific reports* 6, 26138 (2016). [PubMed: 27188985]
82. Farthing D, Sica D, Gehr T, Wilson B, Fakhry I, Larus T, Farthing C, Karnes HT, An HPLC method for determination of inosine and hypoxanthine in human plasma from healthy volunteers and patients presenting with potential acute cardiac ischemia. *Journal of chromatography. B, Analytical technologies in the biomedical and life sciences* 854, 158–164 (2007); published online EpubJul 01 (10.1016/j.jchromb.2007.04.013). [PubMed: 17466604]
83. Schwarzschild MA, Ascherio A, Beal MF, Cudkovicz ME, Curhan GC, Hare JM, Hooper DC, Kieburtz KD, Macklin EA, Oakes D, Rudolph A, Shoulson I, Tennis MK, Espay AJ, Gartner M, Hung A, Bwala G, Lenehan R, Encarnacion E, Ainslie M, Castillo R, Togasaki D, Barles G, Friedman JH, Niles L, Carter JH, Murray M, Goetz CG, Jaglin J, Ahmed A, Russell DS, Cotto C, Goudreau JL, Russell D, Parashos SA, Ede P, Saint-Hilaire MH, Thomas CA, James R, Stacy MA, Johnson J, Gauger L, Antonelle de Marcaida J, Thurlow S, Isaacson SH, Carvajal L, Rao J, Cook M, Hope-Porche C, McClurg L, Grasso DL, Logan R, Orme C, Ross T, Brocht AF, Constantinescu R, Sharma S, Venuto C, Weber J, Eaton K, Inosine to increase serum and cerebrospinal fluid urate in Parkinson disease: a randomized clinical trial. *JAMA neurology* 71, 141–150 (2014); published online EpubFeb (10.1001/jamaneurol.2013.5528). [PubMed: 24366103]
84. Braybrooke JP, Houlbrook S, Crawley JE, Propper DJ, O’Byrne KJ, Stratford IJ, Harris AL, Shuker DE, Talbot DC, Evaluation of the alkaline comet assay and urinary 3-methyladenine

- excretion for monitoring DNA damage in melanoma patients treated with dacarbazine and tamoxifen. *Cancer chemotherapy and pharmacology* 45, 111–119 (2000)10.1007/s002800050018. [PubMed: 10663625]
85. Tittarelli R, Mannocchi G, Pantano F, Romolo FS, Recreational Use, Analysis and Toxicity of Tryptamines. *Current Neuropharmacology* 13, 26–46 (2015); published online Epub01/ [PubMed: 26074742]
86. Holleran WM, Takagi Y, Uchida Y, Epidermal sphingolipids: Metabolism, function, and roles in skin disorders. *FEBS Letters* 580, 5456–5466 (2006)10.1016/j.febslet.2006.08.039. [PubMed: 16962101]
87. Cornejo-García JA, Perkins JR, Jurado-Escobar R, García-Martín E, Agúndez JA, Viguera E, Pérez-Sánchez N, Blanca-López N, Pharmacogenomics of prostaglandin and leukotriene receptors. *Frontiers in pharmacology* 7, (2016).
88. Brereton KR, Green DB, Isolation of saccharides in dairy and soy products by solid-phase extraction coupled with analysis by ligand-exchange chromatography. *Talanta* 100, 384–390 (2012); published online EpubOct 15 (10.1016/j.talanta.2012.08.003). [PubMed: 23141353]
89. Steinberg JG, Delliaux S, Jammes Y, Reliability of different blood indices to explore the oxidative stress in response to maximal cycling and static exercises. *Clinical physiology and functional imaging* 26, 106–112 (2006); published online EpubMar (10.1111/j.1475-097X.2006.00658.x). [PubMed: 16494601]
90. Celi P, Verlhac V, Pérez Calvo E, Schmeisser J, Klunter A-M, Biomarkers of gastrointestinal functionality in animal nutrition and health. *Animal Feed Science and Technology*, (2018); published online Epub2018/07/25/ (10.1016/j.anifeedsci.2018.07.012).
91. Weljie AM, Meerlo P, Goel N, Sengupta A, Kayser MS, Abel T, Birnbaum MJ, Dinges DF, Sehgal A, Oxalic acid and diacylglycerol 36:3 are cross-species markers of sleep debt. *Proceedings of the National Academy of Sciences of the United States of America* 112, 2569–2574 (2015); published online EpubFeb 24 (10.1073/pnas.1417432112). [PubMed: 25675494]
92. Kraeling MEK, Yourick JJ, Bronaugh RL, In vitro human skin penetration of diethanolamine. *Food and Chemical Toxicology* 42, 1553–1561 (2004); published online Epub2004/10/01/ (10.1016/j.fct.2004.04.016). [PubMed: 15304302]
93. Toxicology and carcinogenesis studies of triethanolamine (1999).
94. Wu J, Wang L, Baldwin IT, Methyl jasmonate-elicited herbivore resistance: does MeJA function as a signal without being hydrolyzed to JA? *Planta* 227, 1161–1168 (2008); published online Epub01/23 11/13/received 01/07/accepted (10.1007/s00425-008-0690-8) [PubMed: 18214527]
95. Arya J, Henry S, Kalluri H, McAllister DV, Pewin WP, Prausnitz MR, Tolerability, usability and acceptability of dissolving microneedle patch administration in human subjects. *Biomaterials* 128, 1–7 (2017); published online Epub6// (10.1016/j.biomaterials.2017.02.040.). [PubMed: 28285193]
96. Hastie T, Tibshirani R, Friedman J, *The Elements of Statistical Learning - Data Mining, Inference, and Prediction*. (Springer, ed. Second Edition, 2008).

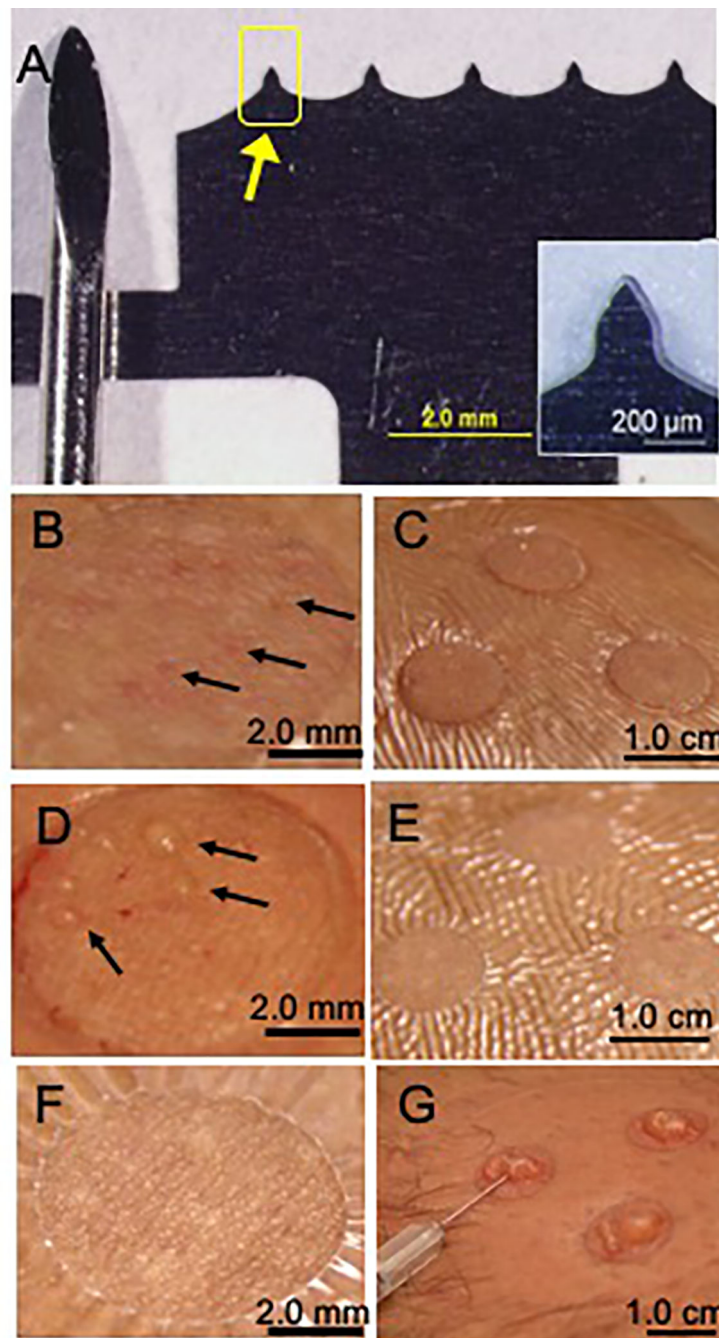


Fig 1. Representative images of microneedle device and interstitial fluid collection by microneedle treatment compared to suction blister.

A. Photograph of stainless steel microneedle (MN) patch (right) shown next to a conventional medium-sized lancet (left). Each of the five MNs (arrow) is 250 μm in length, 200 μm in width at the base and tapering to 10 μm tip diameter. Inset shows a magnified view of a single MN. **B.** Magnified view of skin immediately after MN application. Micropores created from MN-punctured skin appear as faint red dots (arrows). **C.** Skin after MN application and vacuum administration (-50 kPa at room temperature for 20 min) to

draw out interstitial fluid (ISF). Three treatment sites are shown, surrounded by Tegaderm skin covering, before ISF was removed from skin surface. **D.** Magnified view of skin immediately after MN treatment including vacuum administration. Droplets of ISF can be seen on the skin surface above micropores (arrows). **E.** Skin shown 24 h after MN treatment. **F.** Magnified view of skin 24 h after MN treatment. **G.** Photographs of suction blisters formed after extended vacuum application on human skin (-50 kPa to -70 kPa at 40°C for up to 1 h) being drained with a needle and syringe to collect suction blister fluid (SBF). Images (B-E,G) are all from the same subject and are representative of the study population (n=21).

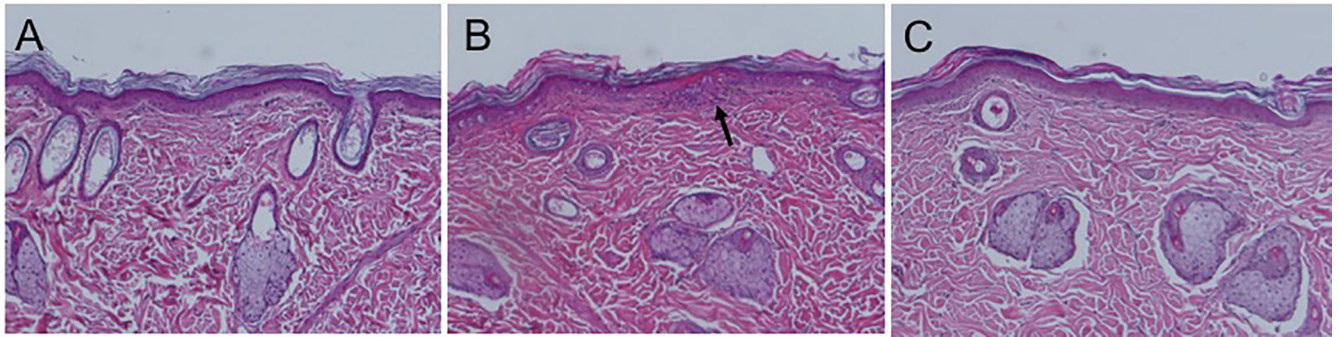


Fig. 2. Representative images of skin from the back of hairless rats before and after in vivo MN treatment.

A. H&E-stained skin section taken from the back before MN treatment. **B.** Histology of skin site taken from a biopsy 4 h after MN treatment. Black arrow shows a site of minor focal inflammation. **C.** Histology of skin 24 h after MN treatment.

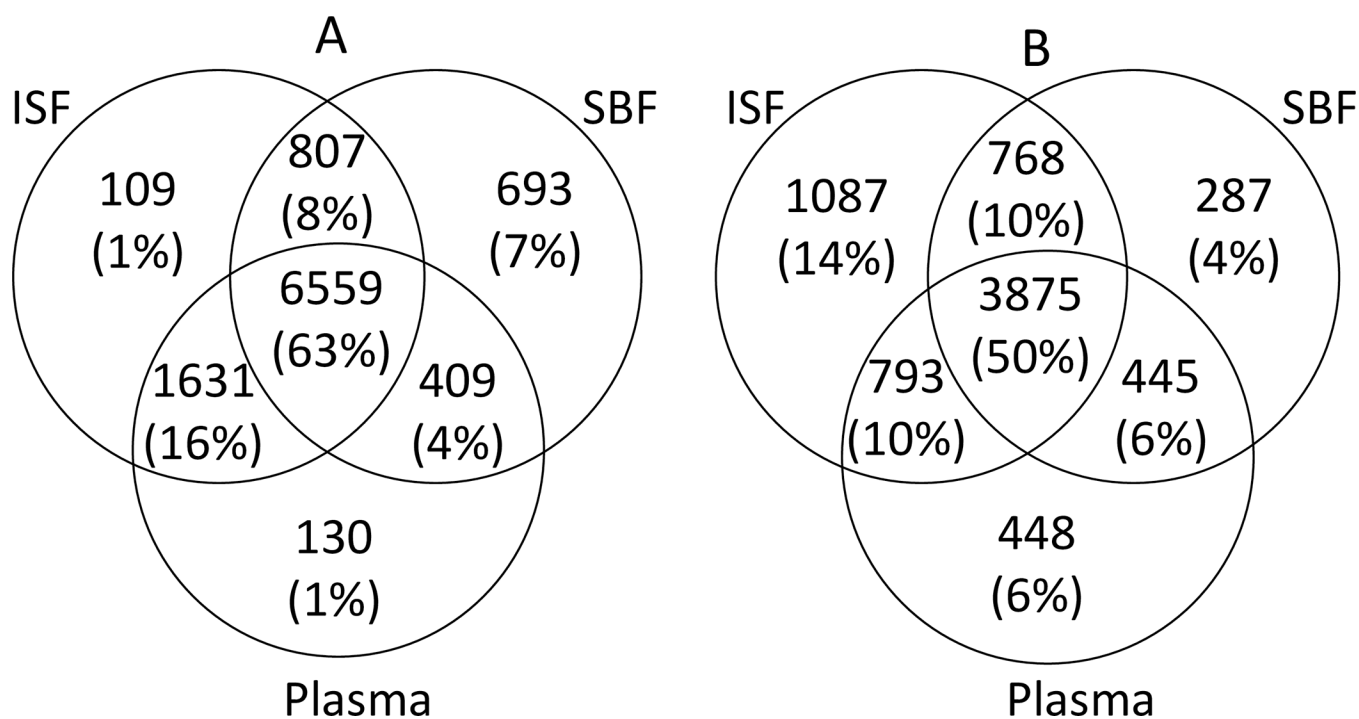


Fig. 3. Venn diagram showing the overlap of features in ISF from MN treatment, suction blister fluid and plasma from venipuncture.

Samples were analyzed using **A.** hydrophilic interaction chromatography (HILIC) and **B.** reverse-phase C18 liquid chromatography. After filtering, a total of 10,338 and 7,703 features were detected with HILIC and C18, respectively. A feature was considered “present” in a fluid if the feature was detected in that fluid in more than 10% of samples (3 of 20 samples). Figures not to scale. ISF, interstitial fluid; SBF, suction blister fluid.

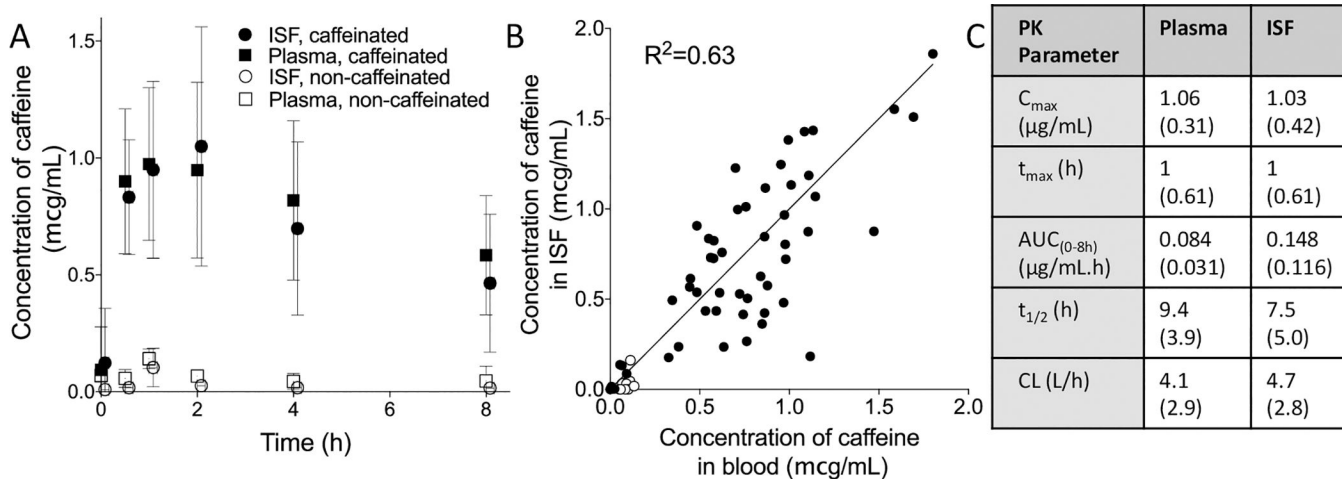


Fig. 4. Concentration of caffeine in ISF and plasma in human participants.

A. Concentration of caffeine in ISF and plasma for 8 h after consumption of caffeinated or caffeine-free soft drink (Diet Coke). Mean \pm standard deviation, $n = 9$. **B.** Correlation between caffeine concentrations in ISF compared to plasma. Each point represents a single time point from a single participant. **C.** Pharmacokinetic parameters for caffeine concentrations in ISF and plasma. All data shown as mean (SD). Log-scale presentation of the data can be found in Fig S18. C_{max} , highest caffeine concentration measured in ISF/plasma; t_{max} , time at which C_{max} was measured; $AUC_{(0-8h)}$, Area under the curve; $t_{1/2}$, half-life; CL, clearance; V_D , volume of distribution

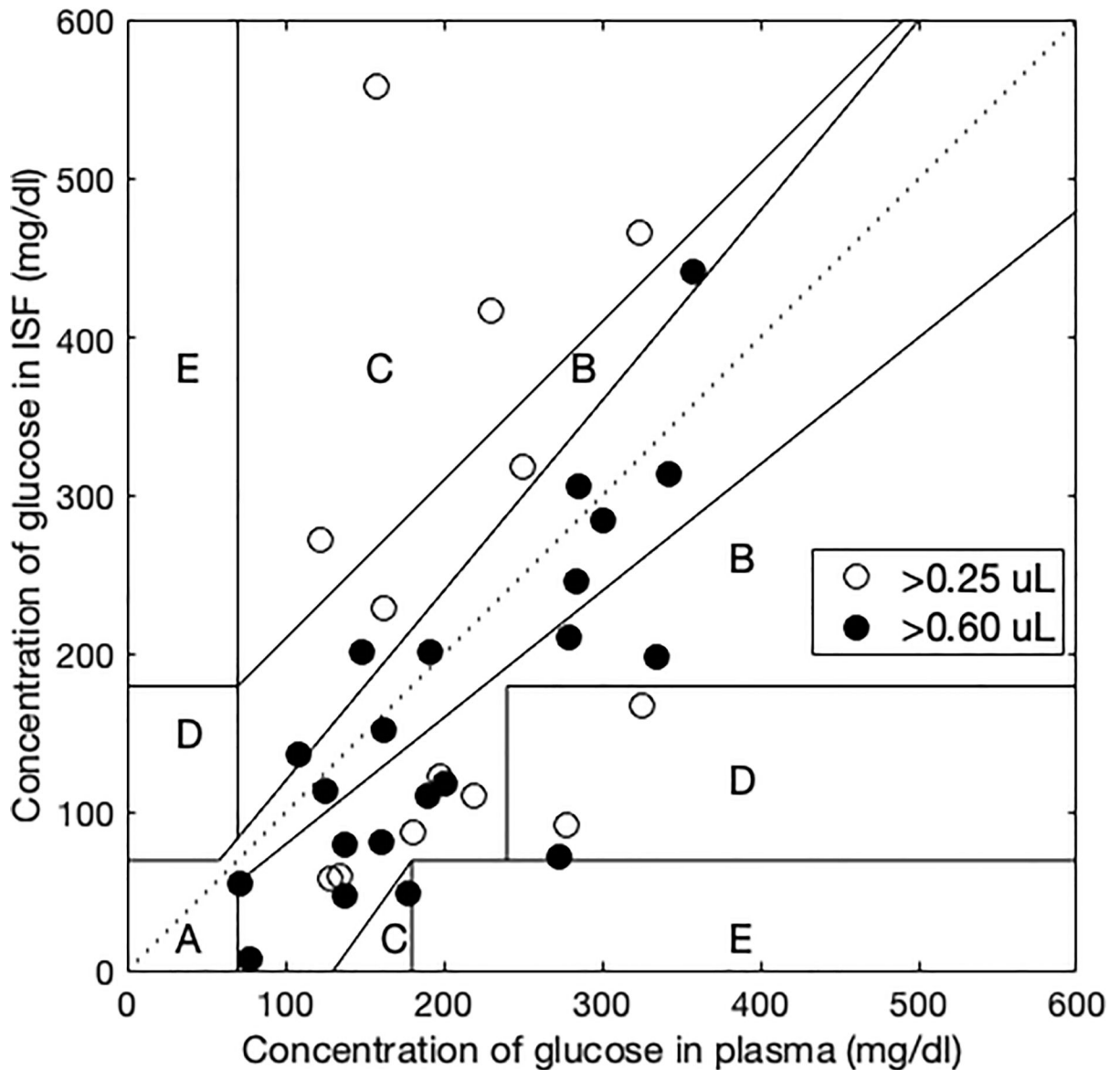


Fig. 5. Clarke error grid showing correlation of glucose concentration in ISF and plasma. Glucose concentration in ISF and plasma were measured in 15 children and young adults with type 1 diabetes before and for 3 h after eating a standard meal. Among ISF samples with volumes $>0.6 \mu\text{L}$ (21 samples from 12 of the subjects) or $>0.25 \mu\text{L}$ (34 samples from 14 of the subjects), 90% or 76% were in the A+B region of the Clarke error grid, respectively.

Table 1.

Prevalence of selected clinically relevant biomarkers in ISF, SBF and plasma in matched samples from 20 human participants.

Biomarker	ID level ^a	Prevalence of biomarker [†]		
		Plasma	ISF	SBF
Clinical Markers				
Bilirubin	1	100%	65%	100%
Carnosine	1	15%	90%	5%
Cortisol	1	100%	30%	80%
Creatine	1	100%	100%	100%
Creatinine	1	100%	100%	100%
Homocysteine	1	20%	55%	55%
Uric acid	1	100%	100%	100%
Vitamins and cofactors				
All-trans-retinoic acid (Vitamin A)	1	85%	90%	25%
Thiamine (Vitamin B1)	1	80%	40%	95%
Lumazine (B2 synthesis intermediate)	1	100%	100%	100%
Pantothenic acid (vitamin B5)	1	90%	65%	100%
Lumichrome (Vitamin B5 derivative)	1	5%	100%	10%
Pyridoxamine (Vitamin B6 form)	1	85%	55%	100%
Pyridoxal (Vitamin B6 form)	1	45%	100%	10%
4-Pyridoxic acid (Vitamin B6 catabolic product)	1	20%	80%	5%
Ascorbic acid (Vitamin C)	1	15%	100%	95%
Ergocalciferol (Vitamin D2)	1	5%	100%	0%
7-Dehydrocholesterol (Provitamin D3)	1	95%	100%	100%
Nucleotide-related metabolism				
Hypoxanthine	1	100%	100%	100%
NAD	1	15%	25%	70%
Uridine	1	95%	100%	100%
Xanthine	1	85%	100%	100%
Fatty acids				
Myristic acid (C14:0)	1	90%	100%	75%
Palmitoleic acid (C16:1)	1	90%	100%	55%
Stearic acid (C18:0)	1	75%	100%	15%
Arachidic acid (C20:0)	1	100%	100%	100%
Sterol metabolism				
Cholic acid	1	90%	95%	100%
Glycocholic acid	1	100%	65%	100%

[†]Prevalence among 20 samples

^aMetabolomics Standards Initiative (MSI) identification confidence level from Sumner *et al.* (71); Refer to table S4 for complete list

Author Manuscript

Author Manuscript

Author Manuscript

Author Manuscript

Table 2.

Prevalence of biomarkers detected uniquely or predominately in ISF compared to plasma in matched samples from 20 human participants.

Metabolite	ID level ^a	Clinical Relevance	Prevalence of biomarker [§]		
			Plasma	ISF	SBF
Amino acid derivatives and metabolism					
Urocanic acid #	1	photocarcinogenesis, UV chromophore(75)	0%	100%	100%
4-Guanidinobutanoic acid	1	biomarker of cirrhosis(76)	10%	100%	90%
Succinylhomoserine	1	biomarker of H1N1-induced pneumonia in mouse model(77)	0%	95%	75%
Vitamins and cofactors					
Lumichrome	2	vitamin B5 derivative	5%	100%	10%
Ergocalciferol	1	vitamin D2	5%	100%	0%
Tocopherol	2	form of vitamin E, micronutrient(78)	5%	100%	0%
Nucleotide-related metabolites					
N6-(delta2-Isopentenyl)-adenine	1	plant growth regulator(79)	0%	100%	85%
Nebularine	2	nucleoside	0%	100%	20%
Cytidine monophosphate (CMP)	1	biomarker of several cancers	10%	95%	100%
Cytidine	1	biomarker of kidney function, several cancers(80, 81)	5%	95%	70%
Inosine #	1	biomarker of cardiac disease (82, 83)	5%	80%	100%
3-Methyladenine *	1	biomarker of DNA damage from chemotherapy(84)	10%	75%	0%
Nicotinamide ribotide	1	agent for diabetes treatment, neuroprotection, anti-aging	0%	50%	100%
Neurotransmitters/Indoles					
N-Methyltryptamine	1	psychoactive alkaloid(85)	5%	70%	5%
Amines					
Sphingosine	2	signaling molecule in skin(86)	10%	100%	50%
Leukotrienes					
20-COOH-Leukotriene B4	2	involved in vasodilation(87)	5%	55%	5%
Carbohydrate metabolism					
Stachyose	1	found in human milk, soy milk(88)	10%	100%	60%
Gulonolactone	2	biomarker of oxidative stress after exercise(89)	0%	100%	10%
Fructose 6-phosphate	1	fructose derivative	0%	85%	100%
Rhamnose	1	biomarker of gut permeability(90)	10%	65%	25%
Organic acids					
Oxalic acid	1	biomarker of sleep restriction(91)	0%	90%	30%
Phosphoenolpyruvic acid	1		5%	85%	100%
Dietary/Xenobiotics					
Diethanolamine *	2	cosmetic formulations, carcinogen(92)	5%	100%	60%
Cyclohexane-1,2-diol	1	cyclohexene oxide metabolite	5%	100%	10%

Metabolite	Prevalence of biomarker [§]				
	ID level ^a	Clinical Relevance	Plasma	ISF	SBF
Triethanolamine # [*]	2	commonly used in skin care products(93)	0%	90%	0%
Methyl jasmonate	1	plant defense chemical(94)	0%	85%	0%

^aMetabolomics Standards Initiative (MSI) identification confidence level from Sumner *et al.* (71)

[§]Prevalence among 20 samples

^{*}Biomarker has dermatological significance.

Author Manuscript

Author Manuscript

Author Manuscript

Author Manuscript